

# A GNC Perspective of the Launch and Commissioning of NASA's SMAP (Soil Moisture Active Passive) Spacecraft

Todd S. Brown<sup>1</sup>

*Jet Propulsion Laboratory, California Institute of Technology, Pasadena, CA, 91109*

The NASA Soil Moisture Active Passive (SMAP) spacecraft was designed to use radar and radiometer measurements to produce global soil moisture measurements every 2-3 days. The SMAP spacecraft is a complicated dual-spinning design with a large 6 meter deployable mesh reflector mounted on a platform that spins at 14.6 rpm while the Guidance Navigation and Control algorithms maintain precise nadir pointing for the de-spun portion of the spacecraft. After launching in early 2015, the Guidance Navigation and Control software and hardware aboard the SMAP spacecraft underwent an intensive spacecraft checkout and commissioning period. This paper describes the activities performed by the Guidance Navigation and Control team to confirm the health and phasing of subsystem hardware and the functionality of the guidance and control modes and algorithms. The operations tasks performed, as well as anomalies that were encountered during the commissioning, are explained and results are summarized.

## Nomenclature

<i>ATE</i>	=	attitude estimator
<i>AU</i>	=	astronomical unit
<i>BAPTA</i>	=	bearing and power transfer assembly
<i>CSS</i>	=	coarse sun sensor
<i>DAFT</i>	=	downlink attitude forecast tool
$\Delta V$	=	change in velocity
<i>FP</i>	=	fault protection
<i>FSW</i>	=	flight software
<i>IGRF</i>	=	International Geomagnetic Reference Field
<i>IMU</i>	=	inertial measurement unit (gyros and accelerometers)
<i>IRU</i>	=	inertial reference unit (gyro)
<i>Izz</i>	=	Z-axis moment of inertia
<i>J2000</i>	=	inertial reference frame
<i>JPL</i>	=	Jet Propulsion Laboratory
<i>FOT</i>	=	flight operations team
<i>MTC</i>	=	magnetic torque controller
<i>MTR</i>	=	magnetic torque rods
<i>NASA</i>	=	National Aeronautics and Space Administration
<i>NAV</i>	=	navigation subsystem
<i>RBA</i>	=	reflector boom assembly
<i>RCS</i>	=	reaction control system (thrusters)
<i>rss</i>	=	root sum square
<i>RTN</i>	=	radial-transverse-normal maneuver definition frame
<i>RWA</i>	=	reaction wheel assemblies
<i>SAA</i>	=	South Atlantic Anomaly
<i>SAR</i>	=	synthetic aperture radar
<i>SEU</i>	=	single event upset
<i>SMAP</i>	=	Soil Moisture Active and Passive

---

<sup>1</sup>Member of Technical Staff, Guidance & Control Formulation and Flight Operations Group, Mail Stop 230-104, Jet Propulsion Laboratory, 4800 Oak Grove Drive, Pasadena, California 91109-8099, USA.

- SPA* = spun platform assembly (the spinning portion of the spacecraft, includes the reflector and boom)
- SPE* = sun position estimation/estimator
- SRU* = stellar reference unit (star tracker)
- TAM* = three axis magnetometer
- TDE* = torque drive electronics

## I. Introduction

ON January 31, 2015, NASA’s Soil Moisture Active Passive (SMAP) spacecraft lifted off from Vandenberg Air Force Base aboard a United Launch Alliance Delta II rocket and was successfully released into a ~690 km polar sun-synchronous orbit.<sup>1,2</sup> Following launch, the SMAP Flight Operations Team (FOT) immediately proceeded to perform vital spacecraft checkout and commissioning activities during the following 3 months, before the spacecraft entered the science phase of the mission. The objective of the SMAP spacecraft is to produce measurements of soil moisture levels in the top 2 inches of soil across the entire globe, and to repeat these global measurements every 2-3 days.<sup>3,4</sup> To accomplish this objective, the SMAP spacecraft includes two science instruments: an L-band radiometer operating at 1.41 GHz, and a tunable L-Band radar operating from 1.22-1.3 GHz.<sup>5,6</sup> The radar is used to produce high spatial resolution measurements but produces only low-accuracy soil moisture measurements, while the radiometer allows for high-accuracy soil moisture measurements, but lacks the spatial resolution of the radar. Together, these science instruments were designed to produce datasets which complement one another and could be combined by ground data post processing to produce the most accurate and up-to-date measurements of global soil moisture levels available from any data source in the world. On July 7, 2015, just 5 months after launch, the SMAP radar suffered an inflight anomaly which rendered the instrument inoperable.<sup>7,8</sup> Investigations into the radar anomaly are ongoing, but in the meantime, the SMAP spacecraft continues to produce global soil moisture measurements using its radiometer instrument.<sup>8</sup>

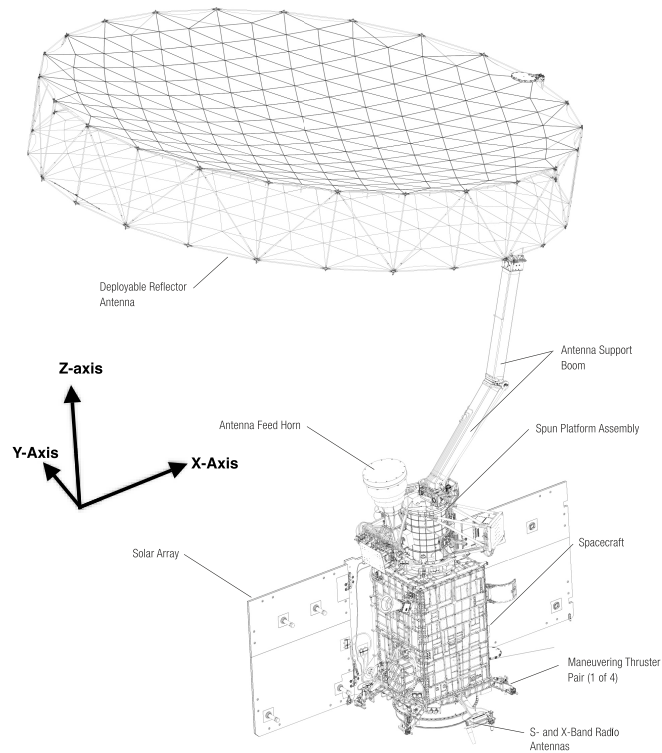


**Figure 1. NASA’s Soil Moisture Active Passive (SMAP) Spacecraft.** *The SMAP spacecraft is shown in the fully deployed science configuration. Note that during normal operations the Spun Platform Assembly, boom, and deployable reflector all spin at 14.6 rpm while the despun portion of the spacecraft maintains three-axis attitude control. All GNC hardware is on the despun portion of the spacecraft. Image courtesy of the SMAP Launch Press Kit<sup>2</sup>*

The value of the soil moisture measurements produced by the SMAP spacecraft was identified by the Earth Science Decadal Survey as being a “national imperative.”<sup>9</sup> The SMAP data will be implemented into meteorological models to improve global weather predictions and will become instrumental in the fields of drought monitoring and flood prediction and mitigation.<sup>1,3,5,6</sup> Despite the excitement surrounding the SMAP launch in the Earth Science community, the science goals of the mission are not applicable to the Guidance, Navigation, and Control (GNC) community, and this paper will instead focus on the GNC challenges of commissioning this Earth orbiting spacecraft.

The SMAP spacecraft and synthetic aperture radar (SAR) were designed and built at NASA’s Jet Propulsion Laboratory (JPL) in Pasadena, CA, with the Goddard Space Flight Center designing and building the radiometer.<sup>4</sup> The SMAP spacecraft was the first Earth-orbiting spacecraft to undergo full spacecraft assembly and system testing at JPL in over 20 years, which made it a significant departure from other more commonly known NASA spacecraft

built at JPL, including the Spirit, Opportunity, and Curiosity Mars rovers, as well as flagship interplanetary exploration spacecraft like Cassini, Galileo, and Voyagers 1 and 2. Nevertheless, the design and testing of the SMAP spacecraft presented unique technical challenges, including a very challenging GNC design, which leant themselves well to JPL's mission of exploration.

The SMAP observatory is a conical-scanning, dual-spinning, 3-axis stabilized spacecraft, where the spacecraft bus holds a fixed attitude relative to the nadir direction, and the science instruments are mounted on a spun platform that rotates at 14.6 rpm (Figure 1).<sup>10,11</sup> The outward appearance of the SMAP spacecraft is dominated by a large 6-meter deployable mesh antenna that is mounted on the spun portion of the spacecraft and on the end of a 5 meter long boom.<sup>12,13</sup> The instrument and Reflector and Boom Assembly (RBA) dwarf the non-spinning portion of the spacecraft. All GNC hardware is mounted on the de-spun portion of the spacecraft. The giant mesh reflector and the conical spin platform are the pieces of technology that allow the radar and radiometer to achieve global coverage with rotating swaths of overlapping instrument data. Although the 6-meter mesh reflector on SMAP is diminutive compared to other commercial satellite deployable reflectors, SMAP may be the only spacecraft to spin such a large reflector while maintaining precise 3-axis attitude control, and therein resides the major GNC difficulty with the spacecraft design.<sup>1,4,12,13,14</sup>

The SMAP spacecraft can maintain attitude control using either a set of eight 4.5 N Reaction Control System (RCS) thrusters, or attitude control can be achieved using a set of four large 250 Nms reaction wheel assemblies (RWA). The RWAs can provide up to an impressive 364 Nms of momentum along the instrument spin axis during normal operations (the RWAs have a great deal of momentum capacity above what can be safely used by the controller), all of this on board a spacecraft with a launch mass of just 944 kg. Although the RCS controller was used for the initial de-tumbling of the spacecraft after launch vehicle separation, as well as attitude control during the first week of operations, the RCS thrusters are now used only for orbit trim maneuvers. Apart from maneuvers and some fault scenarios, the spacecraft attitude will be controlled exclusively by the reaction wheel controller for the remainder of the mission.

For the initial attitude acquisition and for safe mode entries, the SMAP GNC hardware includes two analog Coarse Sun Sensor (CSS) assemblies. Each CSS assembly provides an approximately 120 degree wide (full-cone) field of view where a sun position estimate can be made. One CSS assembly is mounted with the center of its field of view pointed in the same direction as the solar array normal vector, and the 2<sup>nd</sup> CSS assembly is mounted 180 degrees away pointing in the anti-solar array normal direction. SMAP carries three non-articulated solar array panels that all point in the +Y direction (Figure 1). The three-axis attitude estimation logic relies on sensor input data from a Stellar Reference Unit (SRU) as well as an Inertial Reference Unit (IRU). SMAP actually carries two IRU's, though only one IRU can be powered on at any given time. The unpowered IRU is considered an in-flight spare, which has not been powered on since before launch. Being in a 690 km low earth orbit, the SMAP flight software includes a momentum control loop, which uses measurements made by a Three Axis Magnetometer (TAM) to produce commands to send to three Magnetic Torque Rods (MTRs) to actively maintain a zero-momentum state on the spacecraft.

As part of the 90-day spacecraft checkout and commissioning period, the GNC team was required to perform on-orbit checkout and calibration of several pieces of GNC hardware as well as to monitor spacecraft performance as different components of the GNC flight software algorithms were exercised for the first time in flight. The spacecraft commissioning period required GNC support for multiple critical spacecraft events, including: (1) the initial attitude acquisition, de-tumble, solar array deployment, and sun search following launch vehicle separation, (2) the deployment of the large reflector and boom, (3) the orbit trim maneuvers that were used to enter the actual science orbit, and (4) the two stage spin-up of the spun portion of the spacecraft from 0 rpm to 14.6 rpm. This paper will focus on the engineering challenges as well as describe the activities that were performed by the GNC operations team during this eventful commissioning period of the mission.

## II. Launch Vehicle Separation and Initial Sun Search

SMAP launched aboard a Delta II rocket from Vandenberg Air Force Base on 2015-031T14:22:00 UTC, which was on the end of the launch window on the 2<sup>nd</sup> launch attempt. The first launch attempt, on January 29<sup>th</sup>, was scrubbed due to high altitude winds. The SMAP GNC hardware was powered off and the GNC flight software logic was in "Launch" mode, which is an idle mode and GNC was inactive. The spacecraft separation from the Delta II upper stage occurred at 2015-031T15:15:51 UTC, and it was the break wire separation which triggered the SMAP flight software to perform mode transitions which brought the GNC flight software to an active mode.

The immediate responsibility of the GNC flight software after spacecraft separation was to detumble the spacecraft, before entering a planned idle period of several minutes, during which the solar arrays were deployed. After microswitches confirmed the successful deployment of the solar arrays the GNC flight software reentered the detumble mode in order to null any residual spacecraft body rates. The GNC hardware used to support the detumble, sun search, and turn to the Sun included the Coarse Sun Sensors (CSS), the Inertial Reference Unit (IRU), and the RCS thrusters. Since the RCS safe mode controller is the SMAP GNC controller with the greatest control authority, and since the RCS controller is both simpler and more robust than the reaction wheel controller, the initial detumble and sun search were performed on RCS control. Although the operations team expected to see the RCS

thrusters fire to remove tip-off rates following launch vehicle separation, the Delta II upper stage performed an exceptional spacecraft separation where the spacecraft body rates were only  $\sim 0.126$  deg/s, which was well below the flight software threshold to declare the detumble complete prior to any RCS thruster firing. The IRU was powered on and collected 200 Hz gyro and accelerometer data throughout the solar array deployment, which upon later ground review, provided clear indications that both arrays had deployed and locked nominally (Figure 2).

The GNC flight software includes logic which would have performed a four turn Sun Search sequence, including slews of  $+180^\circ$  around Z,  $+180^\circ$  around X,  $+180^\circ$  around Z, and finally  $+140^\circ$  around X in order to guarantee sun vector acquisition. The slew sequence is automatically interrupted upon detection of the sun by the Sun Position Estimation (SPE) logic. Due to the chosen launch vehicle separation attitude, as well as the small tip-off rates, the Sun was immediately detected by the SPE logic using data from the Coarse Sun Sensor assembly, and no Sun Search slews were required. Instead, the spacecraft autonomously performed a  $44^\circ$  slew to point the fixed solar arrays at the Sun. After successfully achieving the power-positive sun-pointed attitude, the spacecraft entered a planned slow roll around the SMAP-Sun vector to guarantee at least intermittent low-rate communication with the spacecraft. GNC hardware and software performance was excellent throughout the initial launch vehicle separation and array deployment, and the operation team's only initial confusion was due to the lack of RCS thruster firing at any point prior to the 44 degree turn to point the solar arrays at the sun. Pre-launch simulations had always assumed "worst case" launch vehicle separation body rates which always required RCS thruster firing, so the operations team was pleasantly surprised to see that the actual detumble and deployment events were much less stressful than planned.

### III. GNC Launch Day Operations

Once the spacecraft achieved the sun-pointed attitude and began the planned slow roll around the sun-line, for GNC the remainder of the flight day was devoted to determining the spacecraft orientation, predicting periods when the spacecraft attitude would be favorable for communication, and monitoring telemetry from the available GNC hardware. During this period of time, the spacecraft had produced a coarse estimate of the sun direction using the sun sensor telemetry, but the star tracker was not initially powered on or producing data, so the spacecraft attitude, while still 3-axis controlled, did not include inertial attitude knowledge.

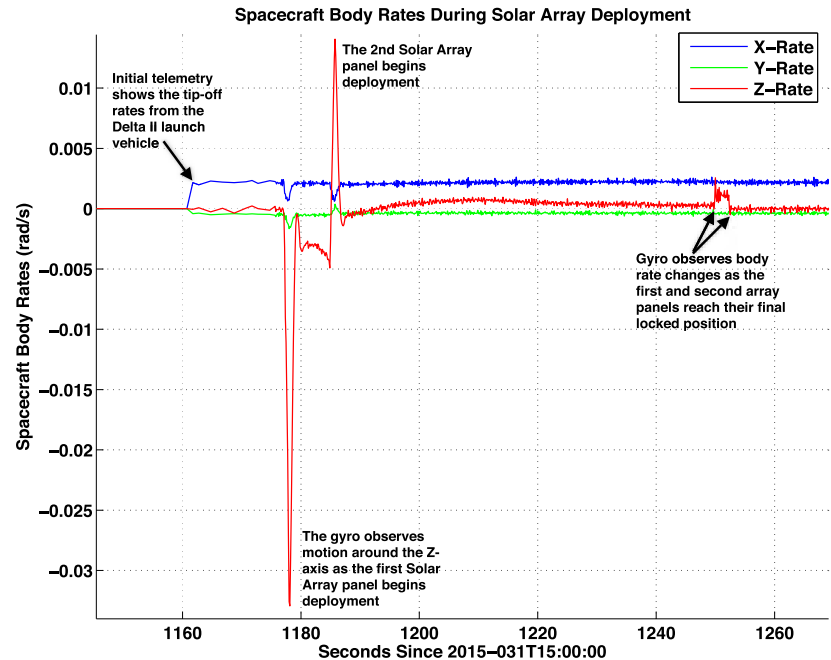


**Figure 2. Spacecraft Body Rates Following Launch Vehicle Separation.** The spacecraft body rates during the solar array deployment provide clear indications of the unlocking and latching events of the solar array panels. Times are UTC.

Although the spacecraft did not need inertial attitude knowledge during the early flight days to maintain the sun-pointed attitude, the inertial spacecraft attitude was required by the operations team for downlink planning. In anticipation of this need, the GNC team developed a ground tool called the Downlink Attitude Forecast Tool (DAFT) to reconstruct the spacecraft attitude on the ground from limited GNC telemetry, and the tool was ready for use at the time of launch. Within the first hour after launch vehicle separation, the operations team powered on two additional pieces of GNC telemetry: the Three Axis Magnetometer (TAM) and the Stellar Reference Unit (SRU). The SRU began producing inertial attitude measurements immediately upon being commanded to acquire stars. To provide an independent verification of the phasing and data quality of the SRU, the inertial attitude of the spacecraft was also reconstructed in real-time from the CSS and TAM telemetry using the DAFT tool. To accomplish this, the SMAP to Sun vector determined by the CSS and the Earth's B-Field vector direction measured by the TAM were compared to the predicted inertial sun direction and Earth B-field direction based on a predicted spacecraft ephemeris and the International Geomagnetic Reference Field (IGRF) model of the Earth. An algebraic attitude estimation (or triad method) algorithm was then used to produce an inertial spacecraft attitude estimate. The SRU-provided attitude estimate was always found to agree with the TAM/CSS produced attitude estimate to within ~3 degrees of error, which was within the expected uncertainty of the TAM/CSS estimation model. In this way, the GNC operations team was able to perform an in-flight demonstration that the SRU was properly phased and producing high quality attitude estimates before the spacecraft transitioned to a mode that used the SRU data. Furthermore, the agreement between the SRU and TAM/CSS attitude estimates demonstrated that the TAM and CSS were also functioning properly and were correctly phased. Using attitude estimates from both the SRU and the TAM/CSS was useful because as the spacecraft was still in a slowly rotisserie roll around the SMAP-to-Sun vector, the SRU was periodically obstructed by the Earth and during those time periods the TAM and CSS-based attitude estimate was the only inertial attitude estimate available.

Launch day did include minor GNC anomalies. Firstly, the +Y facing coarse sun sensor assembly (which points in the same direction as the solar arrays) was observed in telemetry to be much warmer than expected pre-launch due to conservative power generation and consumption estimates. This was quickly determined to be a non-issue since the CSS temperature never exceeded qualification testing limits and no action was required from the team. The second minor GNC anomaly on launch day was due to unexpected SRU behavior. As the spacecraft performed slow rolls around the sun-line the Earth periodically obstructed the SRU. The Earth obstructions were planned, and the pre-launch expectation was that the SRU would immediately recover inertial attitude estimates after the obstruction ended. However, within the first few orbits of the mission, the GNC team determined that following one SRU obstruction by the Earth, the SRU ceased to produce quaternions. Later testing demonstrated that the behavior was repeatable and the SRU would only return to normal attitude estimation if it were reset. During the days following launch, troubleshooting of the SRU by the GNC operations team, the SRU hardware expert, the spacecraft testing and integration team, as well as the SRU hardware manufacturer determined that the unexpected SRU behavior could be avoided using ground commands to change the SRU operating mode prior to each planned obstruction of the star tracker. This workaround requires additional effort by the operations team and remains the planned operations process. The SRU anomaly demonstrated the value of checking out and characterizing the hardware behavior prior to using the hardware in the estimation and control loop. The SMAP GNC team had gone to great lengths to perform end-to-end phasing and functional testing of the CSS, IRU, and RCS thrusters pre-launch since that hardware would be used in the attitude control loops immediately following launch, and the remaining pieces of GNC hardware (the TAM, SRU, reaction wheels, and magnetic torque rods) all received some sort of in-flight checkout prior to use in spacecraft attitude control.

#### **IV. GNC Hardware Checkout and Performance**

The first week of in-flight spacecraft operations was dominated by GNC hardware checkout. The initial spacecraft attitude following launch, which used the slow rotisserie roll around the solar array pointing direction, ensured occasional low-rate communication before the spacecraft had achieved inertial attitude knowledge. However, in order to complete the majority of the spacecraft commissioning activities, the spacecraft needed to maintain the nadir pointed attitude to ensure predictable high rate communication with the spacecraft; this required a full checkout of the SRU hardware. Additionally, the spacecraft continued to use the RCS controller for the first several days of the mission, which used consumables and complicated spacecraft orbit determination. It was therefore also necessary to checkout the reaction wheels, magnetometer, and torque rods so that the spacecraft could begin using the reaction wheel control mode. The spacecraft commissioning plan therefore included time allocation

for the checkout of all GNC hardware during the first week of the mission. This section provides a description of the checkout activities performed for each piece of GNC hardware.

### A. Coarse Sun Sensors

SMAP includes two pyramidal cosine-type analog sun sensor assemblies. Each assembly includes 4 sun sensor heads, each of which contains a single photocell which detects sunlight anywhere within  $85^\circ$  from the sensor boresight. The SMAP Sun Position Estimation logic requires that at least 3 sun sensor heads return output brighter than 25% of the expected maximum solar intensity in order to produce a vector estimate of the sun direction. SMAP includes one CSS assembly which points in the +Y or solar array pointing direction and one assembly pointed in the anti-solar array pointing direction. Baffles are used on each assembly to block glint from the spacecraft structure, and each CSS assembly has an effective half-cone field of view of approximately  $60^\circ$ . Both assemblies received extensive phasing testing in spacecraft integration and system testing during spacecraft assembly. However, the scale factors of the sun sensors were never independently calibrated by JPL after the hardware was delivered by the manufacturer (calibrating the sun sensors is challenging unless you either have a sun simulator which produces light with exactly the same intensity and spectrum of sunlight or are willing to roll your clean spacecraft outside of the clean room into sunlight, which due to the atmosphere is still dimmer than sunlight in low Earth orbit). Since the phasing was already known pre-launch, the in-flight checkout of the CSS assemblies focused on verifying functionality and scale factor calibration.

Immediately after spacecraft separation the telemetry from the Coarse Sun Sensor assemblies showed that there was non-zero output from every single one of the 8 CSS heads. This provided evidence that the hardware had survived launch, but the relative scale factor of each head was still unknown. The four CSS heads aligned with the solar array pointing direction were directly illuminated by sunlight, and could therefore be calibrated relatively easily. The -Y facing sun sensor assembly did not see the sun during the first several weeks of the mission because doing so would require turning the solar arrays away from the sun. However, from launch day onward, the functionality of the -Y facing CSS assembly was known because each of the -Y CSS heads produced current due to reflected sunlight light from Earth's albedo. SMAP's 6:00 am ascending node polar sun-synchronous orbit has the spacecraft flying almost directly over the day/night terminator boundary, which means that the -Y facing CSS assembly generally has line-of-sight to a portion of the Earth that is either in darkness or only receiving twilight illumination, and therefore only a small amount of stray light from Earth reaches the CSS assembly. However, during the solstice seasons the spacecraft does fly over the highly reflective snow and ice at the polar regions while the ground is more directly illuminated by sunlight. Near the northern hemisphere summer solstice the -Y facing CSS assembly registered CSS output values over the North Pole region that were up to 9% of direct solar intensity.

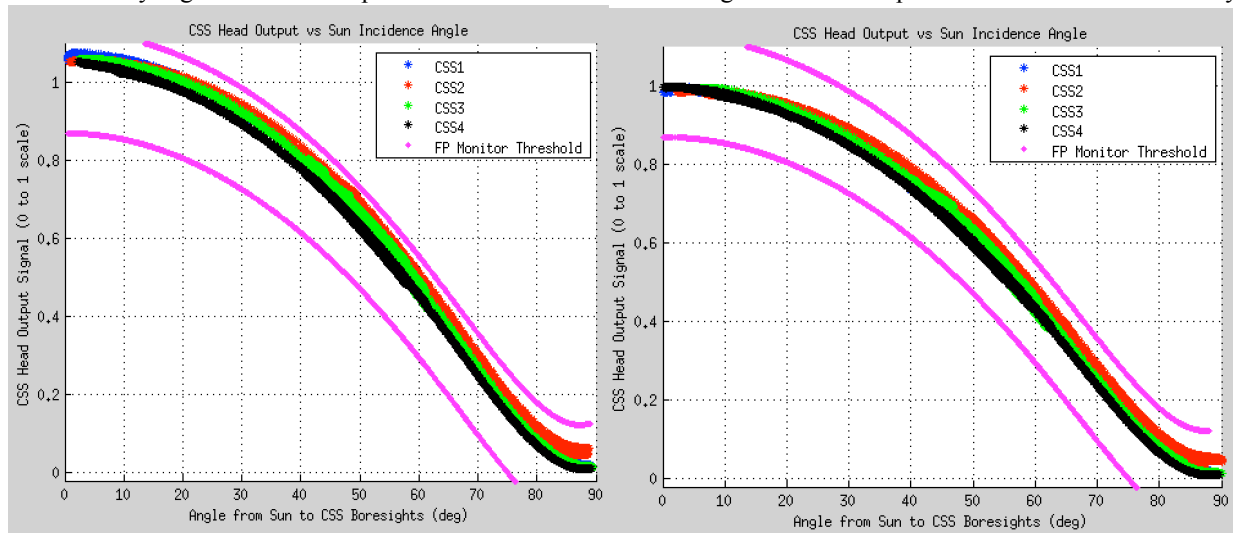


**Figure 3. +Y Facing Coarse Sun Sensor Output Before and After Scale Factor Calibration.** The output of each of the 4 CSS heads on the +Y facing CSS assembly are plotted as a function of the angle between the CSS head boresight and the direction to the Sun. Sunlight directly along the boresight of one CSS head should produce an output of 1.0 for a properly set scale factor. A depiction of the approximate acceptable operating envelope is shown with two magenta lines, defining an upper and lower limit to the output. Prior to the CSS scale factor update (left) the output of each of the 4 heads was higher than 1.0 for small angles, and after the scale factor update (right) the CSS output falls in the middle of the desired operating envelope.

The reflected light from Earth reaching the +Y facing CSS assembly is certainly larger than the amount reaching the -Y facing assembly, but is more difficult to distinguish from the incident sunlight.

The hardware manufacturer had calibrated the scale factors of each CSS head pre-launch and the flight software parameters specified that direct sunlight on any of the CSS heads at 1 AU from the sun should produce an output signal of 1.0 (non-dimensional). As previously noted, the +Y facing CSS assembly is at a much higher in-flight temperature than was expected pre-launch; the +Y CSS assembly reached temperatures as high as 113° C. Due to the warmer than expected CSS operating environment, the CSS heads on the +Y CSS assembly produced more current than expected, and therefore needed an in-flight scale factor parameter update. The +Y CSS scale factors were calibrated using a series of spacecraft slews which swept the sun from ~0-90 degrees from each of the four CSS heads' boresights. As a result of the calibration, +Y facing CSS heads had their full solar intensity scale factors increased by [7.1, 6.1, 6.3, 5.1] %, respectively, for the four CSS heads. The scaled CSS output from the four heads on the +Y assembly are shown both before and after the update in Figure 3. The magenta lines show an approximation of the envelope of expected CSS output variability allowed within the flight software (FSW)<sup>15</sup>, and the observed telemetry from each head is shown across the full range of possible illumination angles. Prior to the scale factor update, the output of all four heads was biased closer to upper end of the magenta envelope, and after the update the telemetry falls almost exactly in the middle, as intended.

During the Low Rate Spinup activity, which will be discussed later, the spacecraft bus counter-rotated and sunlight shone directly onto the -Y side of the spacecraft for the first and only time since launch. During the Low Rate spinup, the four heads on the -Y facing CSS assembly received direct sunlight and produced output that was consistent with the pre-launch scale factor, since the -Y CSS assembly is in a much cooler operating environment than the +Y facing assembly. For this reason the -Y facing CSS assembly has not received a scale factor update in-flight.

## B. Inertial Reference Units

The SMAP spacecraft includes two inertial reference units, though only one can be powered on at a time. IRU-A is the only IRU that has been used in-flight, and there are no plans to ever exercise IRU-B in-flight for any reason other than a major anomaly, which is not anticipated. The SMAP IRU's are both inherited from other JPL projects; IRU-A was a piece of backup hardware procured for JPL's Juno mission, which will arrive at Jupiter in 2016, and IRU-B was used for field testing of the Mars Science Laboratory (Curiosity) entry descent and landing system. Both IRUs were refurbished and recalibrated for SMAP during spacecraft development.

The SMAP IRUs are actually "IMUs" (inertial *measurement* units) and do include 3-axis accelerometers in addition to the 3-axis gyroscopes. Although the IRU accelerometers function and produce telemetry, the data from the accelerometers is not used by any piece of the GNC flight software. The operations team has commanded the spacecraft to collect high-rate gyro and accelerometer data during dynamic spacecraft events for later ground analysis, but only the gyro data is used inside the GNC flight software algorithms.

Both IRU's received end-to-end phasing testing pre-launch because the hardware was used in the control loop during the initial spacecraft detumbling and sun search turns. For this reason, the primary purpose of the in-flight calibration for the IRU was to determine the functionality/aliveness of the hardware following launch and to determine the relative misalignment between the IRU and SRU. Fine-tuning the alignment of the IRU relative to the SRU was necessary to ensure the spacecraft attitude knowledge met science pointing requirements during SRU outages caused by occasional moon occultations, which can last up to ~10 minutes. One of the planned commissioning activities was a sequence of multiple ~40 degree slews that the spacecraft executed around the X, Y, and Z axes. The slew sequence was a GNC activity that was designed to provide the data necessary to determine inertia properties of the fully deployed spacecraft and also to allow for the calibration of the misalignment between IRU-A and the SRU. Based on the results of the in-flight calibration of the alignment of IRU-A to SRU, only a small alignment update of 0.07° was determined to be needed. Although the IRU-A alignment update was minor, the change still resulted in a noticeable estimator improvement. The Attitude Estimator (ATE) flight software includes logic to estimate the IRU error. The estimated error includes components from gyro bias, scale factor error, and misalignment. The estimated IRU error telemetry is shown in Figure 4 for the period of time that includes the IRU-A alignment parameter update. During period shown in Figure 4, the spacecraft is maintaining the nadir pointed attitude and is otherwise quiescent, so the change in the estimated gyro error telemetry shown in Figure 4 is entirely due to the improvement of the IRU-A alignment parameters. IRU-B has not received an in-flight alignment calibration because the backup hardware cannot be powered on. If IRU-B is ever promoted to be the prime IRU, it will receive a similar calibration.

In addition to calibrating the IRU-A alignment, the IRU-A scale factor error was also roughly estimated in-flight. There was no specific commissioning activity planned to calibrate the IRU scale factor error. However, there have

been multiple occasions following spacecraft launch and safing events where the spacecraft attitude knowledge was performed via gyro propagation for periods as long as several days. During these gyro propagation periods, the SMAP operations team would opportunistically power-on the SRU so that inertial attitude estimates were available in telemetry, even while the SRU data was not being used in the control loop. During these periods of time, it was possible for the GNC team to compare how the gyro-propagated attitude was drifting relative to the SRU inertial measurements. In this manner, the IRU-A attitude propagation error was determined to be 0.30 degrees/day, and this is believed to be primarily due to IRU-A scale factor errors, along with small contributions from the gyro bias and residual misalignment errors.

Although the IRU accelerometer data is not used in the GNC flight software, the data has proven to be highly beneficial to the operations team for ground analyses. The deployments of the solar arrays, the reflector boom assembly, and the

deployment of the mesh reflector itself were all events that were difficult to observe using engineering telemetry. All of the deployments were planned to be confirmed using microswitch states or cable tension telemetry. However, the ability of the IRU to collect >8 Hz accelerometer and gyro data for later downlink and processing proved highly useful in confirming nominal deployment events, observing pyro firings events, and also in reconstructing  $\Delta V$  maneuver magnitudes. Examples of the IRU accelerometer accuracy will be shown later.

The SMAP spacecraft did experience one autonomous IRU reset activity, which resulted in a spacecraft safing event. A thorough review by the operation team and hardware manufacturer concluded that internal IRU logic behaved correctly in resetting itself as a response to detecting a corruption in the IRU avionics, presumably caused by an SEU. The internal actions of the IRU, as well as the FSW Fault Protection response, successfully restored the IRU to working order within several seconds, and IRU-A has continued to function normally since that time. The primary lesson learned by the operations team from the IRU reset was the need for the spacecraft flight software to include logic which can allow for the graceful handling of autonomous GNC hardware activities similar to the IRU reset. This lesson applies to both the IRU and SRU, as will be described later.

### C. RCS Thrusters

The SMAP RCS controller consists of eight 4.5 Newton RCS thrusters. Four of the RCS thrusters are mounted so they provide thrust in the +Z direction (Figure 1) and these thrusters fire in pairs to produce torque around either the spacecraft  $\pm X$  or  $\pm Y$  axes. Since all four Z-facing RCS thrusters point in the +Z direction, they cannot fire as opposing couples to produce pure torque, and they instead produce torque while also imparting  $\Delta V$  to the spacecraft. The other four RCS thrusters are aligned with the spacecraft  $\pm Y$  axis (Figure 1) and fire as opposing couples to produce pure torque around the  $\pm Z$  spacecraft axis. The Y-facing thrusters do not impart any significant  $\Delta V$  when they fire. For  $\Delta V$  maneuvers the spacecraft will enter a mode where all four +Z facing thrusters are turned on simultaneously and then individual thrusters are off-pulsed in order to maintain attitude control during the maneuver. The RCS thrusters are fed from a single blow-down tank of hydrazine monopropellant pressurized with helium. SMAP launched with 81 kg of propellant, of which only 5.3% has been consumed as of October 2015.

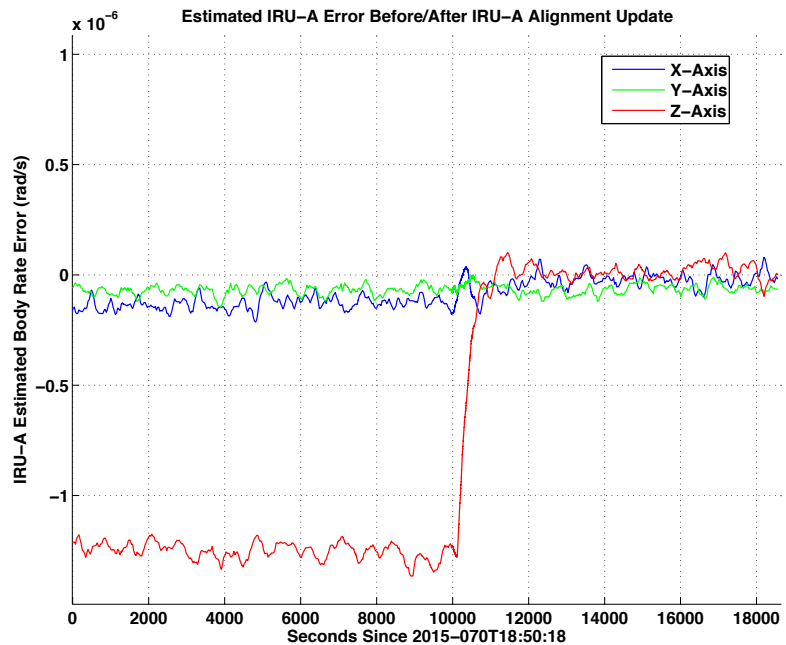


**Figure 4. Estimated IRU-A Rate Error During IRU Alignment Parameter Update.** The plot shows the ATE estimate of the IRU-A body rate error per axis as a function of time. The IRU-A estimated error includes components of bias, scale factor error, and misalignment. The IRU-A alignment parameter is instantaneously updated at  $t \approx 10,000$  seconds on this plot and following the update the estimated Z-axis gyro error is dramatically improved. The spacecraft maintained a quiescent nadir pointed attitude throughout this time period. Times are UTC.

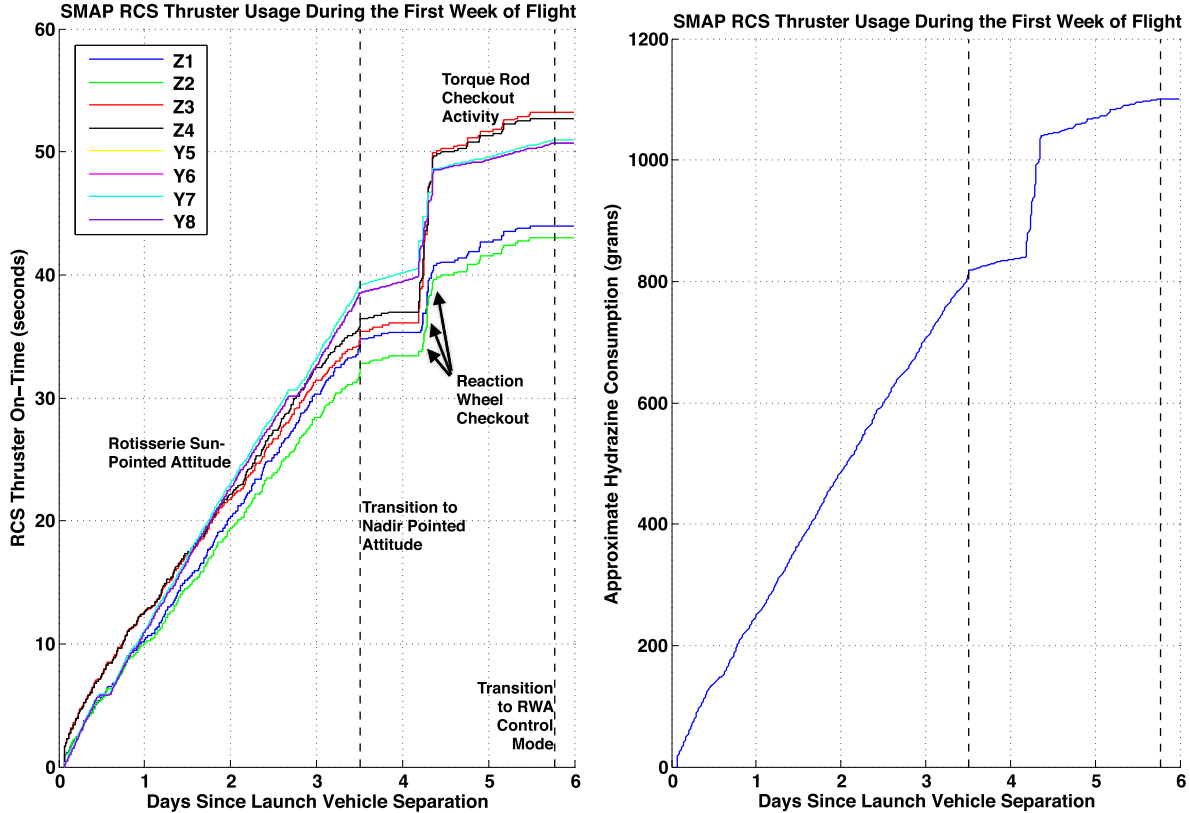


**Figure 5. RCS Thruster Usage During the First Week of Flight.** The RCS thruster on-time (left) and estimated hydrazine consumption (right) are shown for the first six days of the SMAP mission. During the first 3.5 days the spacecraft remained at the sun-pointed rotisserie roll attitude, before the spacecraft transitioned to the normal nadir pointed RCS control mode. Of the hydrazine consumed while at the nadir-pointed attitude, the majority was due to the RWA checkout activity and torque rod checkout activity. The quiescent hydrazine consumption rate is significantly lower while at the nadir pointed attitude than in the rotisserie sun pointed attitude.

As previously described, the RCS controller was used to maintain attitude control during the first 6 days of the mission following launch. However, since the spacecraft first transitioned to RWA control on Flight Day 6, the RCS thrusters have only been used during planned  $\Delta V$  maneuvers. Since the RCS thrusters received rigorous end-to-end phasing in pre-launch testing of the spacecraft, the primary purpose of checking out the RCS thrusters was to confirm that all of the thrusters were still functioning after launch, and to gauge the hydrazine monopropellant consumption rate for both the rotisserie attitude (where the spacecraft slowly rolled around the SMAP-to-Sun direction) and during the normal nadir pointed RCS control mode. For both RCS control modes the attitude controller maintained the attitude errors within a 15 degree per-axis deadband.

Telemetry showing the RCS thruster on-time as well as an estimate of the hydrazine consumption during that period are shown in Figure 5. To maintain the rotisserie sun-pointed attitude, the RCS attitude controller consumes a total of 83 seconds of RCS On-Time per day, which amounts to 211 grams of hydrazine per day. The steady-state quiescent hydrazine consumption for nadir-pointed RCS control was far more efficient at 11.5 seconds of RCS on-time per day and 31 grams of hydrazine consumed per day. The nadir pointed RCS control mode is more efficient because the spacecraft was designed to have lower gravity gradient and aerodynamic external torques when the spacecraft is at the nadir pointed attitude. The periods of increased hydrazine consumption while the spacecraft was at in the nadir pointed RCS control mode were due to checkout activities of the reaction wheels and torque rods, both of which imparted a significant amount of torque to the spacecraft. Examples of RCS thruster performance for  $\Delta V$  maneuvers are shown later.

#### D. Magnetic Torque Rods and the SMAP Momentum Control Loop

The SMAP GNC flight software actively maintains the total system angular momentum. Nominally, the SMAP spacecraft maintains a zero momentum state, though it is possible to add a momentum bias if the operations team ever desired to have one. The momentum control loop consists of a momentum estimator and a momentum

controller. The momentum estimator sums the angular momentum contributions of (1) the despun portion of the spacecraft body, (2) the spun platform assembly (SPA is shown in Figure 1), and (3) the RWAs. The momentum controller computes the difference between the desired momentum state and the estimated momentum state in order to determine the momentum error. The momentum controller then uses telemetry from the three axis magnetometer (TAM) to determine the direction of the Earth's external magnetic field and then commands voltages to the three torque rods as required for the external magnetic field and the MTR magnetic moment to impart a torque that reduces the total spacecraft system momentum. The momentum control loop therefore requires spacecraft body rate and inertia information, spun instrument assembly spin rate telemetry and inertia information, RWA spin rate telemetry and inertia properties, as well as magnetometer telemetry in order to function properly. A lack of any of these pieces of information could force the spacecraft to transition to RCS control, and potentially to spin-down the spun platform assembly (SPA), though fortunately, this has never occurred in flight.

The GNC hardware includes three 230 A-m<sup>2</sup> magnetic torque rods (MTRs) used to load and unload spacecraft momentum. Each of the three MTRs is aligned with one of the spacecraft body axes. The magnetic moment of the torque rods is *not* varied by applying variable voltage to the torque rod, but rather the imparted torque from the MTR's is varied by changing the MTR duty cycle (i.e. the proportion of time the torque rod is on). Each 10 seconds the GNC momentum control goes through a full cycle where during the first second all 3 torque rods are producing no torque and the telemetry from the magnetometer is read to determine the external magnetic field. During the 2<sup>nd</sup> through 10<sup>th</sup> second of the momentum control loop the torque rods receive a command to "fire" from anywhere between 0 and 9 seconds, based on the size of the current momentum error. Note that a torque rod "firing" refers to the process of applying a voltage to the torque rod (i.e. energizing the MTR) in order to produce a magnetic moment for a fixed period of time. Although the torque rods can use a 100% duty cycle when momentum is commanded to be added or removed from the system, the torque rods are typically fired well below a 1% duty cycle when the SPA is spinning and the despun spacecraft is quiescent and maintaining the nadir attitude. Each torque rod can be

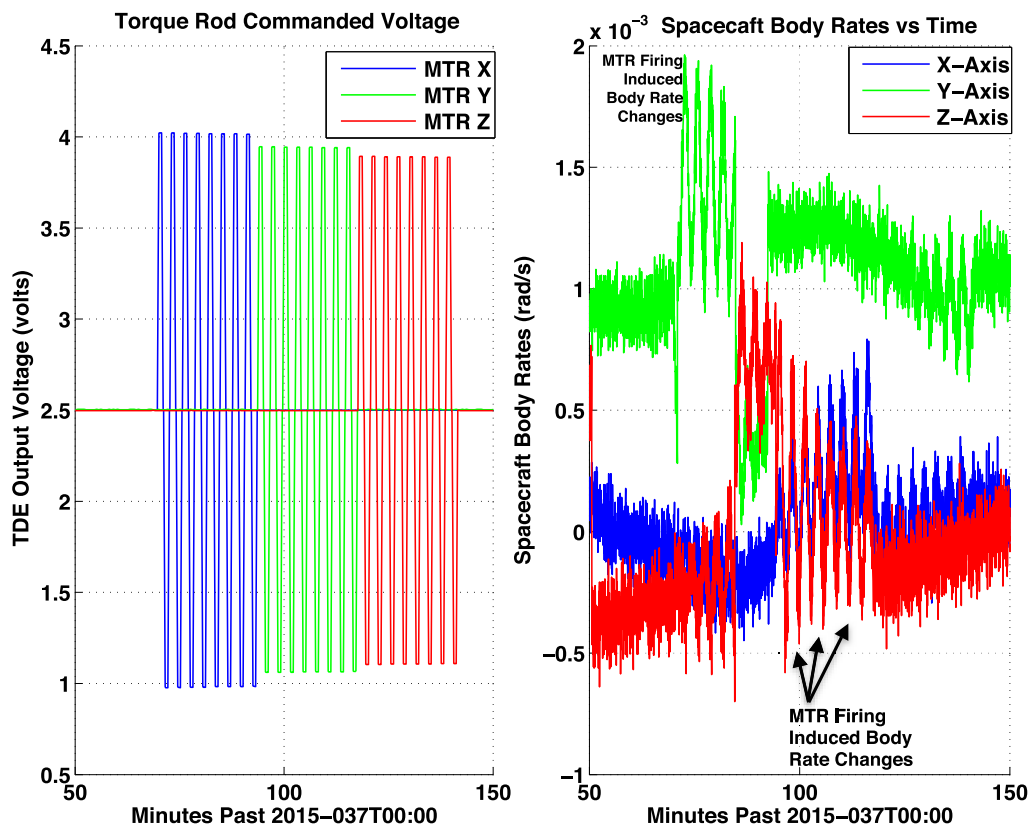


**Figure 6. Flight Telemetry from the MTR Checkout Sequence.** *The telemetry showing the commanded voltage being applied to each of the torque rods is shown in the left-hand plot while the resulting spacecraft body rates for this time period are shown in the right hand plot. During this period the spacecraft was under RCS control at the nadir pointed attitude. Instantaneous large changes in spacecraft body rates are due to RCS thruster firing, but the short period oscillatory changes in the body rate telemetry are due to the torque resulting from the MTR firings. Times are UTC.*

commanded to produce either a positive or negative magnetic moment.

The primary purposes of the MTR hardware checkout during the SMAP commissioning were to demonstrate hardware functionality and also to confirm that the MTRs were properly phased. To accomplish this, an MTR checkout sequence was designed pre-launch, which would issue a set of commands to the torque rods to apply alternating positive and then negative magnetic moments for 60 consecutive seconds followed by 30 seconds without any MTR firing. Each torque rod was tested individually in this way over the course of the sequence (Figure 6). The sequence duration was chosen so that the commands to each torque rod spanned the amount of time required for the spacecraft to fly between the equator and the pole, so each torque rod was seen to fire in both polarities over a 90 degree range of Earth latitudes. The ground team could then use both the TAM telemetry, which easily detects the torque rod firings, as well as the spacecraft body rate and attitude control error telemetry in order to confirm that the direction of the commanded magnetic torque was the same as the achieved magnetic torque. Due to the large size of the SMAP MTRs, the effects of the MTR firings can be easily resolved in the attitude control telemetry while the spacecraft maintained its normal RCS controlled nadir pointed attitude. Body rate and attitude errors could be observed between the infrequent RCS thruster pulses. Figure 6 depicts the spacecraft telemetry returned during the MTR checkout activity. The voltage applied by the Torque Drive Electronics (TDE) in the left plot shows the commanded MTR firing and the spacecraft body rates during the MTR firings is shown in the right hand plot. The short period of scalloping visible in the spacecraft body rate telemetry is a change in the spacecraft rotation rate due to the torque from the MTR firing as the spacecraft drifts between RCS thruster control pulses. One might wonder if the scalloped shape of the body rate telemetry is indicative of real spacecraft motion or whether it could be due to electromagnetic interference from the energized torque rods. However, the independent telemetry from the TAM, Sun Sensors, and SRU all confirmed that the MTR firings caused real spacecraft motion.

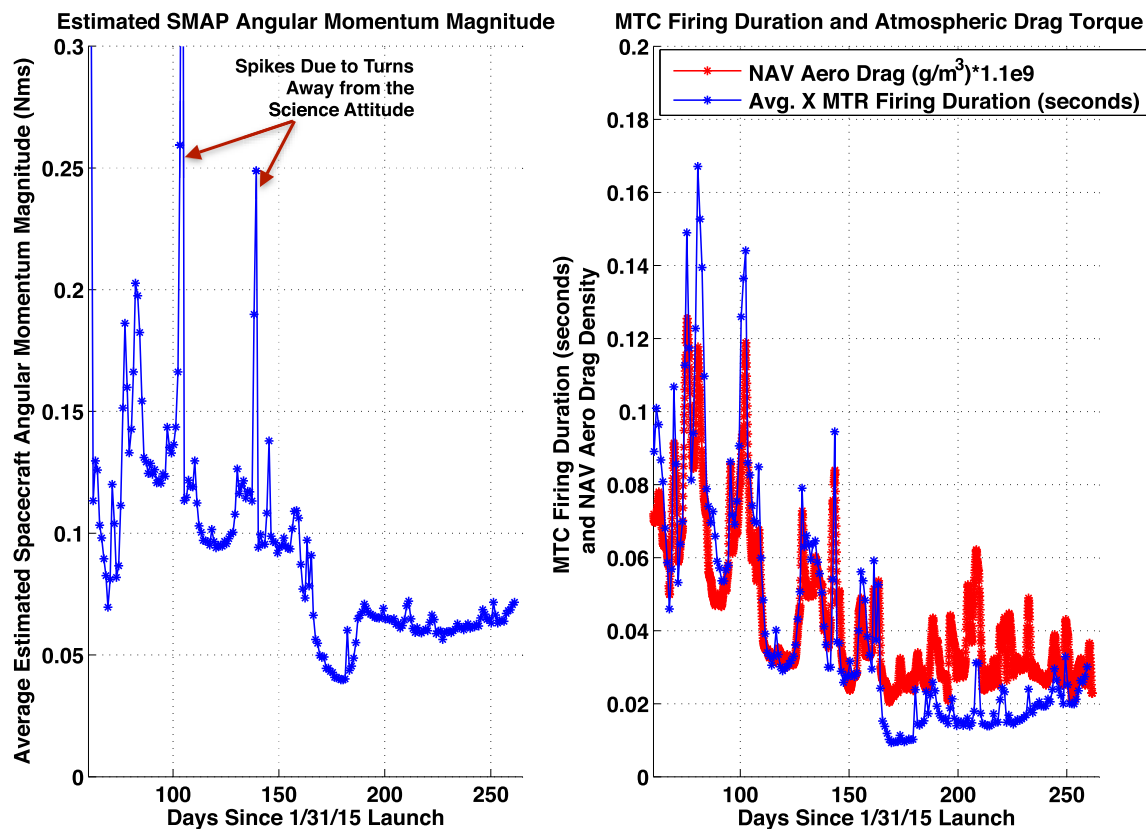


**Figure 7. SMAP Angular Momentum Vector Magnitude and Average X-axis MTC Firings Duration Compared to Aero Drag Density.** The left-hand plot shows the estimated daily average angular momentum vector magnitude of the SMAP spacecraft system, which includes the spacecraft body rates, RWA spun inertia, and SPA spun inertia. The net system momentum is typically less than 0.1-0.2 Nms. The right hand plot compares the daily average X-axis MTC firing duration in seconds, where the MTC firing duration could be any duration between 0-9 seconds. The Navigation team's estimated atmospheric/aerodynamic drag density is shown scaled by an arbitrary scale factor so that it overlies the GNC telemetry. The average X-axis MTC firing duration is clearly correlated to atmospheric drag density.

In that way, the phasing and functionality of each torque rod was confirmed.

The momentum state of the spacecraft was variable in the early phases of the spacecraft commissioning as the spacecraft transitioned between RCS and RWA control, occasionally disabled momentum control for some checkout activities, and even temporarily added a momentum bias for the gyroscopic stiffness during the deployment of the boom and reflector. However, after the spacecraft completed the spin-up to the 14.6 rpm science spin rate and began science operations, the momentum state of the spacecraft stabilized at a nearly zero value. The spacecraft momentum controller is a proportional controller that attempts to maintain the zero momentum state. However, imperfections in the FSW knowledge of the inertia of the SPA and true mechanical spin axis, as well as external torques on the spacecraft result in the spacecraft carrying a small, but non-zero, momentum that is typically less than 0.2 Nms of inertial angular momentum (Figure 7). The estimated system angular momentum is controlled with brief torque firings commanded to each of the MTRs.

The operations team noticed large day-to-day variations in the average magnetic torque controller (MTC) firing duration for the torque rods aligned with the spacecraft X and Z axes, and the GNC team determined that the variation was primarily due to changes in the aerodynamic torque on the spacecraft from Earth's tenuous upper atmosphere. The right-hand plot of Figure 7 compares the daily average X-axis MTC firing duration to the scaled atmospheric density. The density of Earth's upper atmosphere varies due to changes in space weather (i.e. coronal mass ejections, solar flares, and geomagnetic storms) and imparts a time varying aerodynamic drag torque on the spacecraft. The atmospheric disturbance torque is primarily imparted around the spacecraft Y-axis, due to a non-zero offset in the YZ plane between the spacecraft center of mass and the center of pressure. Since the atmospheric density estimated by the SMAP Navigation team has vastly different units ( $\text{g/m}^3$ ) compared to the average MTC firing duration (seconds), the atmospheric density data in Figure 7 as been artificially scaled by an arbitrary constant so that the datasets overlay one another. Although Figure 7 only shows the data for the X-axis aligned torque rod, a similar trend is also visible in the data for the Z-axis aligned torque rod, though no such trend appears in the telemetry of the Y-axis aligned MTC. Figure 7 clearly shows that increased atmospheric drag is correlated to increased MTC firing durations and increased system momentum, though the momentum controller still easily bound the momentum growth.

### E. Three Axis Magnetometer

As described in the previous section, SMAP's Three Axis Magnetometer (TAM) is used in the momentum control loop to determine the direction of the external magnetic field so that the momentum control logic can determine which combination and polarity of torque rod firings should be commanded to reduce residual angular momentum. The TAM was powered off at the time of launch vehicle separation because the spacecraft was using the RCS controller and the momentum control loop was inactive. The TAM was powered on shortly after launch, along with the SRU, so that the GNC team could determine the inertial attitude of the spacecraft based on raw telemetry from the SRU as well as the TAM and CSS. As previously described, the ground-computed inertial attitude of the spacecraft using only TAM and CSS data agreed with the inertial attitude estimate returned by the SRU to within 2.5 degrees. That analysis, performed in real time on launch day using the DAFT ground tool, demonstrated that the TAM had survived launch and was producing data that was properly phased.

The primary purpose of the checkout of the TAM hardware during commissioning was to determine whether a large deterministic TAM bias was present in the TAM telemetry, because the GNC flight software included the ability to correct for a body fixed TAM bias. A sufficiently large TAM bias could prevent the spacecraft from effectively maintaining a zero momentum state. To test for the presence of a bias, the ideal telemetry for use comes from extended periods of time where the TAM produces telemetry while flying over large ranges of Earth latitudes, while the torque rods are inactive. During commissioning, the most suitable period of time to perform a TAM bias calibration occurred during the first week of flight, while the spacecraft was at the nadir pointed attitude but still using the RCS control mode and the torque rods were powered off. The calibration activity compared the TAM B-field measurement to the IGRF model predict of the Earth's B-Field vector at the location of the spacecraft based on a predicted spacecraft orbit ephemeris. In Figure 8, the per-axis difference between the TAM measured B-field and the predicted B-field from the IGRF model is shown as a function of spacecraft latitude. The difference between TAM and IGRF model B-Fields is as large as ~3000 nano-Tesla, but even this amount never exceeds 8% of the measured B-field magnitude. Similarly, the angular difference between the TAM measured B-field vector and the IGRF predict ranges from 0 to 3.8 degrees, with the maximum angular error occurring when the B-field is weakest over the equator. Of the estimated TAM error, a portion corresponds to true TAM bias and scale factor error and a portion is due to modeling error. An estimate of the TAM bias can be computed by finding the average per-axis TAM error for the data shown in the left-hand plot of Figure 8. For the data from Oct 12, 2015, which is shown in Figure 8, this bias was computed to be  $[X, Y, Z] = [-443 \ -160 \ -402] \text{ nT}$ , which is comparable to, though slightly

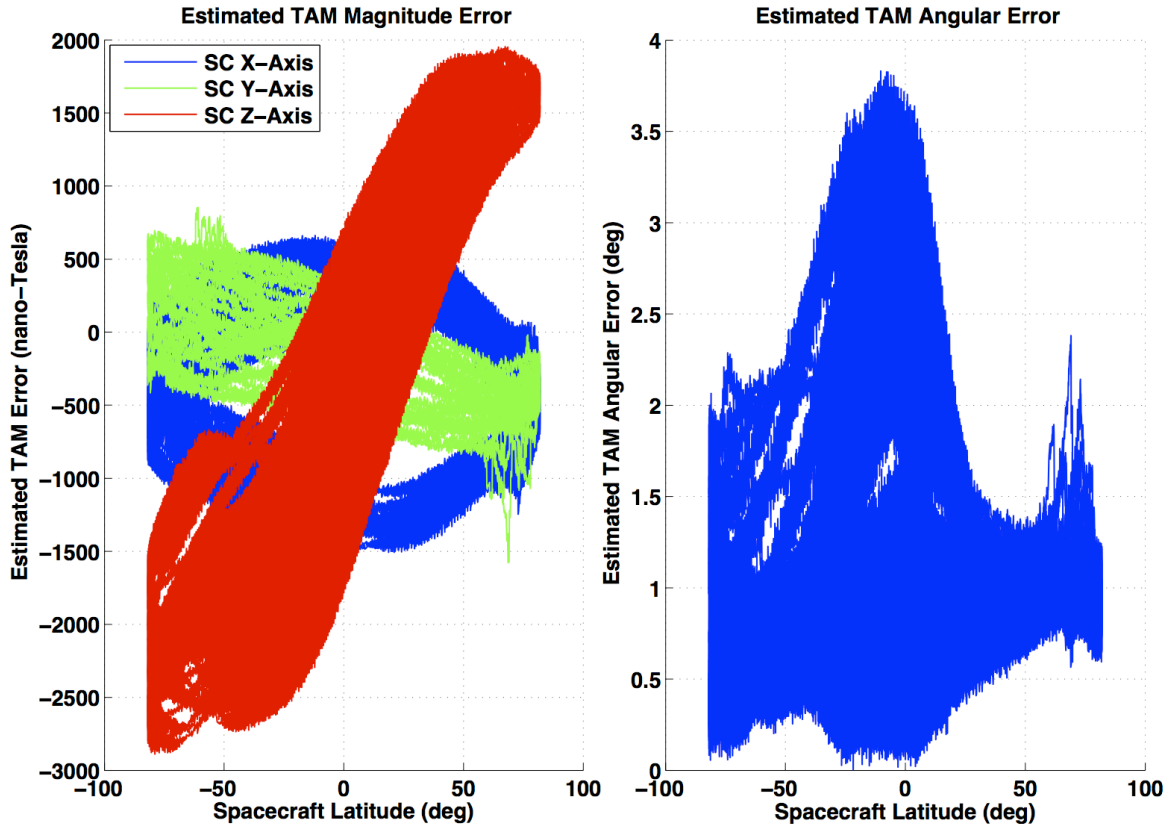


**Figure 8. In-Flight Estimation of Three Axis Magnetometer (TAM) Error.** *The TAM telemetry for a 24 hour period spanning Oct 12, 2015 is mapped to the spacecraft body frame and compared to the predicted magnetic field magnitude and direction based on the ground based IGRF model and the spacecraft ephemeris as a function of spacecraft latitude in its polar orbit around the Earth. The left-hand plot shows the difference between the measured and expected magnetic field shown per axis. The right hand plot compares the angular difference between the B-field vector direction measured by the TAM and the B-Field vector direction expected based on the IGRF model. The TAM error is plotted as a function of spacecraft latitude because there is an obvious correlation between the two.*

larger than, the magnitude to the TAM bias computed after launch on Feb 4, 2015:  $[X, Y, Z] = [-379 \ -37 \ -356]$  nT. The difference between the estimated biases is insignificant considering the intra-day variability in the TAM vs. IGRF data, and both estimates are far smaller than the 3000 nT requirement on TAM bias control. Since the SMAP TAM is only required to be coarsely calibrated in order for the momentum control logic to successfully maintain the system angular momentum, the operations team has chosen not to update the TAM bias parameters onboard the spacecraft, and to instead continue to monitor the TAM bias for any change.

## F. Reaction Wheel Assemblies

The SMAP spacecraft carries four 250 Nms reaction wheel assemblies. The RWAs are mounted on the spacecraft to provide significantly more angular momentum capacity along the spacecraft Z-axis, in order to counter the angular momentum of the Spun Platform Assembly (SPA). When the SPA is spinning at the full 14.6 rpm science spin-rate, the angular momentum of the SPA is 359 Nms along the spacecraft Z-axis, and yet the spacecraft is required to fly in the zero momentum state. For that reason, during science operations, the RWAs are at spin rates of  $[RWA1, RWA2, RWA3, RWA4] = [2330, 2240, 2245, -2700]$  rpm in order to produce an angular momentum that exactly counters the momentum of the SPA. The RWA hardware allows spin-rates up to 6000 rpm, and the wheels were tested to this rate on the ground, but the SMAP FSW includes multiple fault protection monitors that limit the effective spin rate to  $\pm 4500$  rpm. None of the RWAs has spun faster than 2880 rpm at any point in the mission.

One of the SMAP RWAs (RWA4) has a spin axis exactly aligned with the spacecraft Z-axis, but is mounted upside down relative to the other 3 RWAs. The other three RWAs (RWA1, RWA2, and RWA3) are mounted such

that their spin axes are exactly 30 degrees from the spacecraft Z-axis and are equidistant from one-another. Since four wheels are used in the RWA controller, and since all 4 wheels have linearly independent spin axis directions, the RWA controller has one degree of freedom in selecting the RWA spin-rates to produce a desired momentum state. Generally, when the SPA is spinning at the 14.6 rpm science spin rate, the RWA controller keeps the RWA spin rates nearly balanced. However, when the SPA is not spinning the operations team commands the RWA controller to force RWA4 to +850 rpm, while still maintaining a zero net momentum state; doing so forces RWA1, RWA2, and RWA3 to spin up to ~350 rpm. This commanding is performed so that none of the RWAs is forced to spend long periods of time at a spin-rate very close to 0 rpm. Spin-direction reversals, also known as zero-crossings, cause transient spikes in the RWA attitude and rate control errors that are undesirable, and are therefore avoided.

SMAP does not carry a backup reaction wheel, so the failure of even one reaction wheel would have a significant impact on the ability of the spacecraft to perform normal science operations, and for this reason the operations team has a strong incentive to closely monitor the health and functionality of the reaction wheels in order to determine whether there are any alarming trends in the reaction wheel telemetry.

The SMAP RWAs underwent extensive ground testing prior to launch, so the primary purpose of the in-flight checkout of the RWAs was to confirm that the RWAs were properly phased, and to confirm that the reaction wheels survived the spacecraft launch without any noticeable degradation. Since the spacecraft used RCS control during the first week after launch, it was possible for the operations team to individually test the functionality of each of the RWAs before the spacecraft began using the RWAs for attitude control. The in-flight RWA checkout consisted of

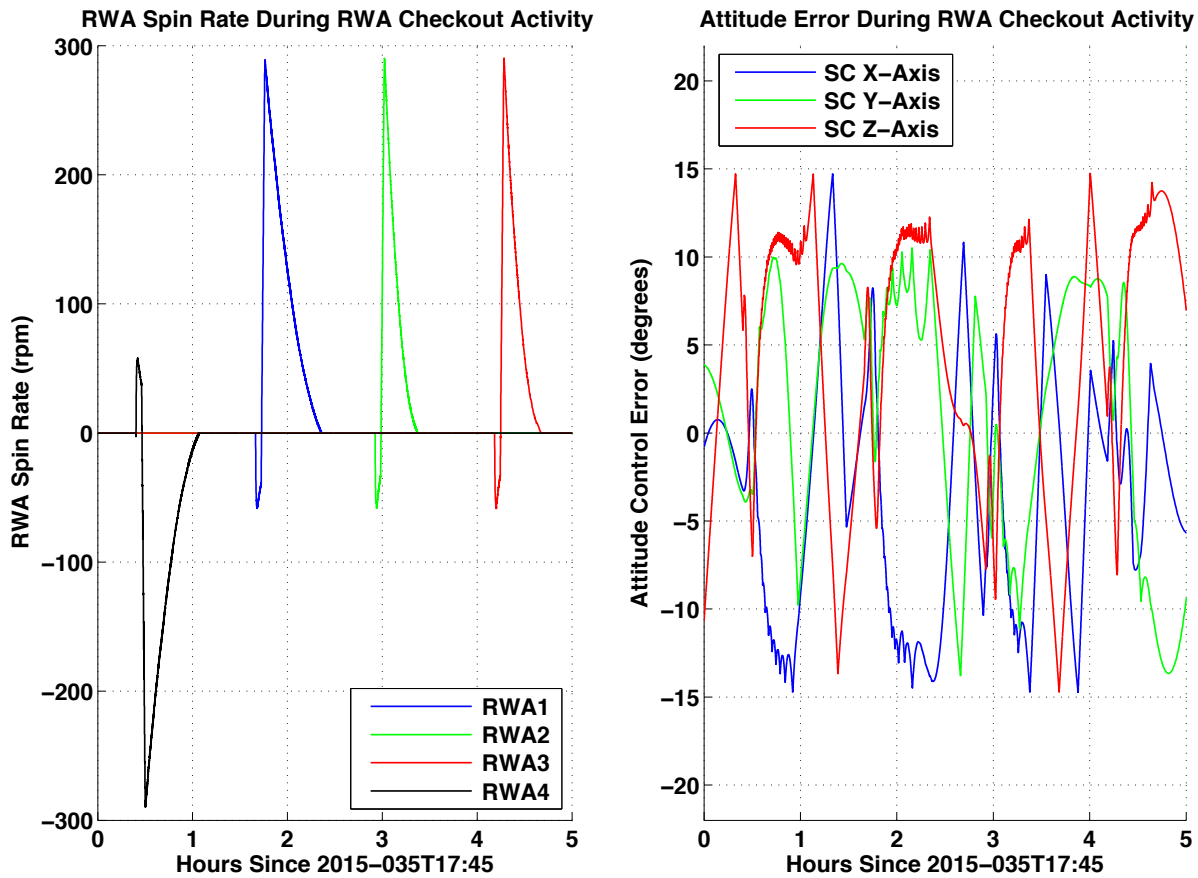


**Figure 9. Reaction Wheel Spin Rate and Attitude Error Telemetry During RWA Checkout Activity.** *The left-hand plot shows the RWA spin-rate telemetry. During the RWA checkout activity each RWA was commanded to -60 rpm and then +300 rpm (RWA4 received the opposite commands because it is mounted upside down relative to the other 3 RWAs), and then the RWA was allowed to coast down from 300 to 0 rpm. The right-hand plot shows the attitude control error estimated by the RCS attitude controller during the RWA checkout activity. RCS thruster pulses were used to maintain the attitude error within a  $\pm 15$  degree deadband. The scalloped edges of the attitude control error during periods where the RWA was accelerating/decelerating can be used to determine the direction of the applied torque from the wheel, and therefore the RWA spin-direction phasing can be confirmed. Times are UTC.*

the RWAs individually receiving open loop commanding to first accelerate to -60 rpm (negative denotes counterclockwise rotation) and then to +300 rpm (Figure 9). Note that in Figure 9, RWA4 received polarity commands opposite of the other 3 RWAs because RWA4 is mounted upside down relative to the other RWAs. After reaching ~300 rpm the torque to the RWAs was disabled and the reaction wheel were free to coast-down to 0 rpm. The sequence that performed this test was designed to take minimal time while allowing an independent check that each wheel was free to rotate in both directions, and give a baseline estimate of the RWA bearing drag torque based on the coast down. The spacecraft attitude control telemetry collected during the period when the RWAs were accelerating, or decelerating was used as an independent verification that the RWA spin-direction was producing the expected torque on the spacecraft, and were thereby phased correctly. An inspection of the attitude control error included in Figure 9 shows that X and Z axis attitude errors were obviously affected by the torque from the RWAs.

Since the initial RWA checkout, the operations team has accumulated ~250 days of continuous RWA telemetry, of which 80% was spent with the spacecraft maintaining the nadir pointed science attitude while the SPA was spinning at 14.6 rpm. During science operations, the RWA spin-rates vary by no more than ~5 rpm, which is less than 0.3% of the total spin rate of each RWA. The nearly constant RWA spin-rates allows for long term trending of the estimated RWA drag torque for each RWA, as shown in Figure 10. The data plotted begins at Day 56, following

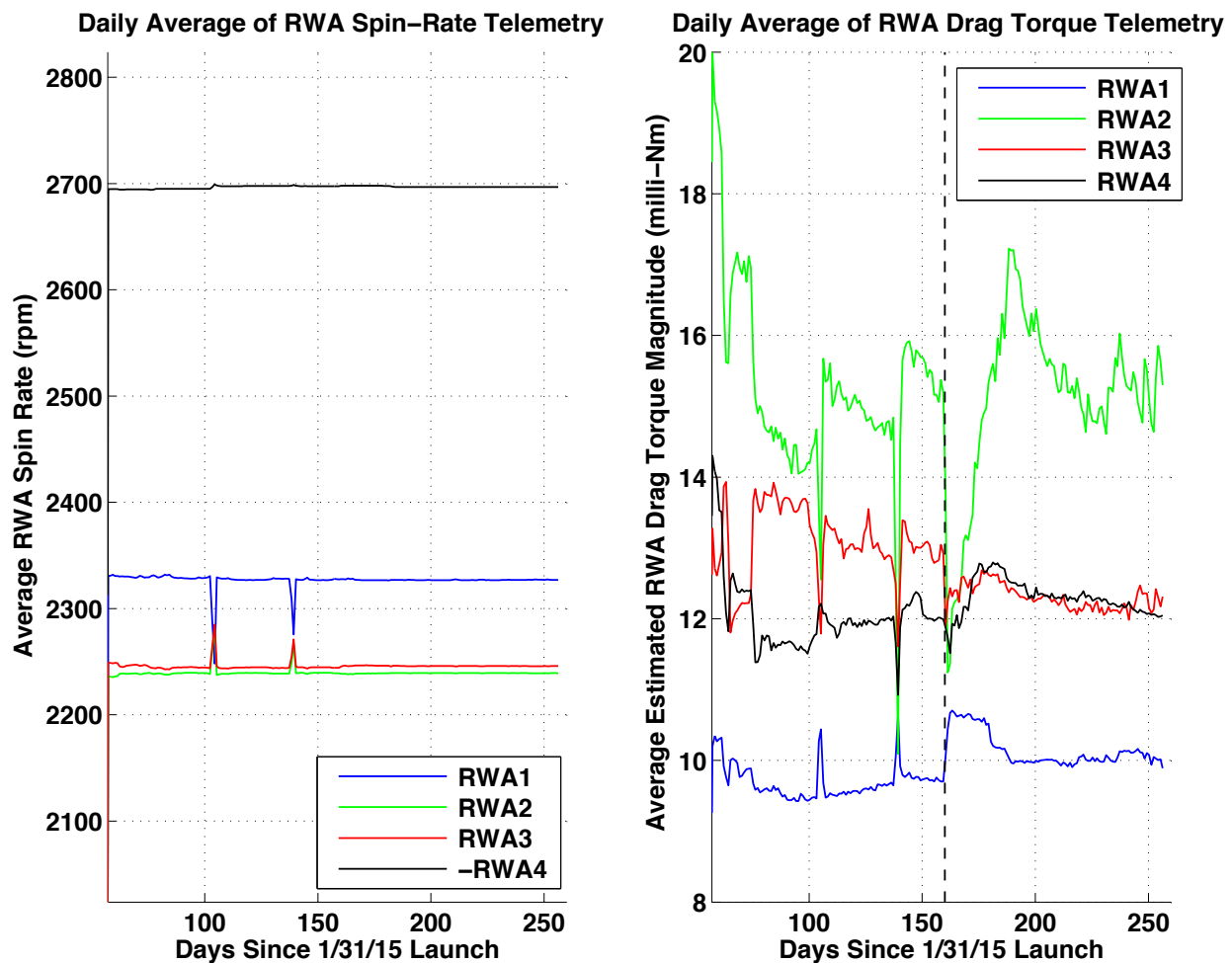


**Figure 10. Reaction Wheel Spin Rate and Drag Torque Telemetry.** The left-hand plot shows the daily average of the RWA spin-rate telemetry for each of the four RWAs during 200 days of science operations. The right-hand plot contains the magnitude of the daily average estimated RWA drag torque telemetry for the same time period. Note that the RWA4 spin rate was artificially reversed since the wheel is mounted upside-down relative to the other wheels. Spikes in the RWA1-3 spin-rate telemetry correspond to dates when the spacecraft was briefly at the safing attitude rather than the nadir pointed attitude. The vertical dashed line on the right-hand plot denotes the date of the radar anomaly, which caused an abrupt cooling in the RWA operating temperature, explaining the visible drag torque transient.

the spin-up of the SPA. In Figure 10 RWA spin-rate telemetry and estimated RWA drag torque telemetry have been split into 24 hour-long segments and the average RWA spin-rate and average RWA drag torque during each day is computed and included in the plot. Since RWA4 is mounted upside-down relative to the other RWAs, it actually has a negative spin-rate, which was manually negated for better visibility alongside the other RWAs.

During the time period plotted in Figure 10, large changes in the average estimated RWA drag torque are visible for each of the RWAs, but most of these changes are correlated to transient events. Some of the most significant transients in Figure 10 include: Days 104 and 139, when the spacecraft was briefly at the safing attitude, and Day 160 which is highlighted with a vertical dashed line for additional visibility. Day 160 of Figure 10 corresponds to the data when the SMAP radar instrument encountered an anomaly that rendered the SAR unable to transmit.<sup>7,8</sup> The SAR anomaly had no direct impact on GNC performance, but did cause large changes in the operating temperature of the RWAs, which were mounted close to the radar electronics inside the spacecraft. For that reason, the change in RWA drag torque telemetry to the Day 160 event can be entirely attributed to the varying thermal environment, rather than changes inherent to the RWAs themselves. Although there is some wheel-to-wheel variation in average RWA drag torque levels, as of October 2015 the GNC operations team sees no worrisome trends in the available telemetry, though diligent monitoring will continue for the length of the mission.

A close inspection of the RWA spin-down testing in Figure 9 shows that the spin-down from RWA1 and RWA4 took longer than the spin-down from RWA2 and RWA3, which confirmed pre-launch testing that showed RWA1 and RWA4 experienced lower levels of drag torque than did RWA2 and RWA3. The long term drag torque telemetry shown in Figure 10 confirms that RWA1 continues to show lower drag torque than the other wheels, and although RWA4 shows drag torque comparable to other wheels, RWA4 is actually spinning 450 rpm faster than the other three and therefore RWA4 actually does still have lower drag than both RWA2 and RWA3.

### **G. Stellar Reference Unit**

The SMAP spacecraft carries a single Stellar Reference Unit (SRU), which is mounted on the spacecraft such that the SRU optics are pointed nearly in the anti-velocity direction of the spacecraft, though the SRU boresight is tipped up in the +Z direction by ~30 degrees to keep the SRU field of view unobstructed by the Earth when at the nadir attitude. The SMAP SRU performs the star pattern identification internally and provides a J2000 to SRU quaternion as part of its output telemetry. The SRU is more complicated than the other GNC hardware in that it includes its own software, processor, memory, and state machine, and as a result, the GNC subsystem has more star tracker related telemetry than is available for any other GNC hardware. Due largely to the complexity of the SRU itself, as well as the SRU data handling, the SMAP spacecraft avoids using the SRU in the attitude control logic in all safe modes, and the SRU was powered off during the initial launch vehicle separation and sun search.

Like the other GNC hardware, the primary purposes of the SRU hardware checkout following launch included confirming the hardware survived the launch environment and also confirming that the SRU quaternions were properly phased. In addition, the GNC checkout activities included an SRU photo sequence in which the SRU was placed into a photo mode where subsets of the SRU pixel data could be directly collected for inspection on the ground to confirm that the SRU field of view was unobstructed, free of contaminants, and that SRU images contained identifiable star patterns. The photos collected demonstrated that the SRU was clear of any discernable obstructions. SRU phasing was confirmed on launch day using the procedure described in Section III, to compare the SRU attitude estimate to the TAM/CSS derived attitude estimate.

Following launch, the SMAP SRU immediately began to report an unanticipated error condition quite regularly. The SRU has the ability to detect when there is an excess of star-like objects in the SRU images, and when an excessive number of objects are detected the SRU reports an “excess stars” type condition in its telemetry, though SRU performance is unaffected by the error condition and attitude estimation is still possible. The locations of the SMAP spacecraft at the times when the SRU reported the excess star error condition are shown in Figure 11. The data plotted in Figure 11 was drawn from four months of flight telemetry, spanning from June – October 2015, and during this period the SRU reported >201,000 instances of these “excess stars” errors. The SRU reported the excess star conditions so often that the GNC team was able to correlate the events to external error sources: first, the excess stars condition can occur if the SRU is obstructed by the Earth while attempting to acquire an inertial attitude estimate, though this condition does not occur during normal science operations and there are no such examples in Figure 11. Second, the SRU “excess stars” error can be triggered by the moon passing through the SRU field of view, which does occur regularly during science operations. In Figure 11 many examples of SRU “excess stars” errors triggered by moonlight in the SRU images are visible over the mid southern latitudes. Thirdly, during the northern hemisphere summer the operations team observed SRU “excess stars” errors being reported during periods of elevated background image noise due to stray light from the Earth’s brightly illuminated north polar region. Although the SRU hardware includes a baffle designed to reject stray light, the operations team presumes that there

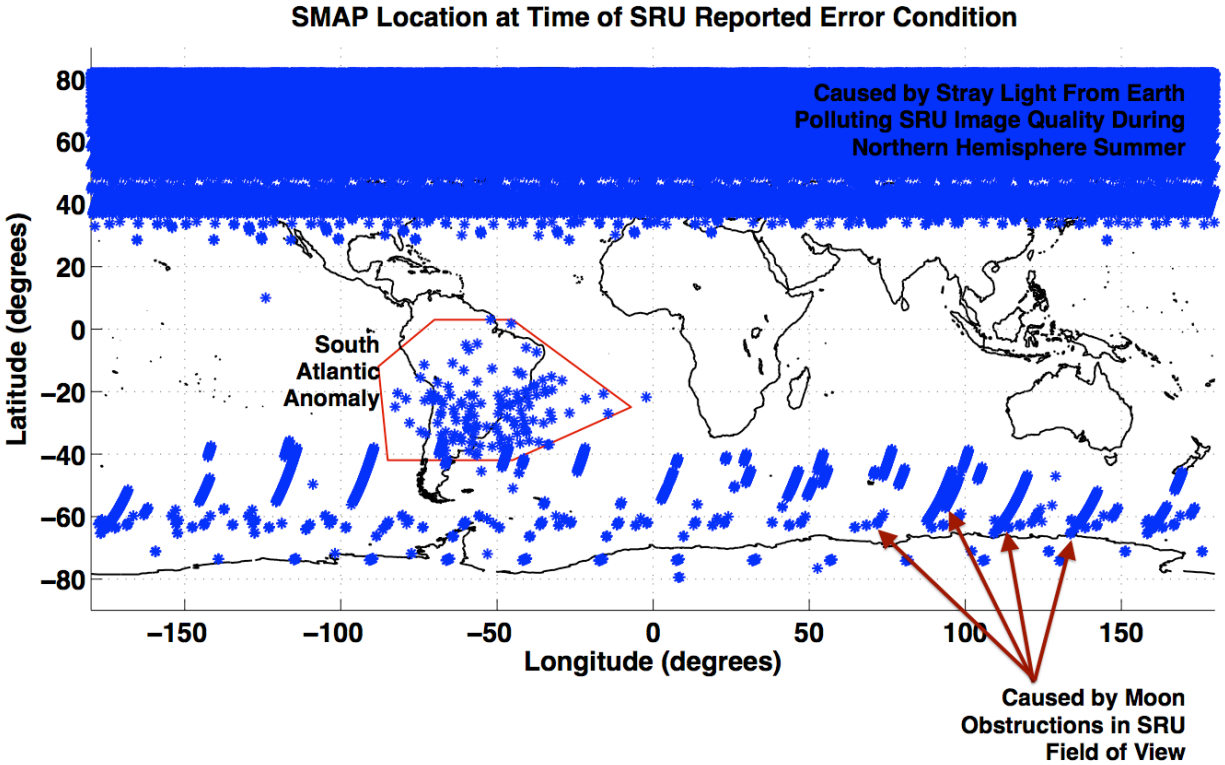


**Figure 11. Location of SMAP Spacecraft When SRU “Excess Stars” Errors Reported.** *Between 6/8/15 and 10/19/15 the SMAP SRU reported >201,000 instances of errors caused by an excessive number of star-like objects in the SRU images. The majority of these star-like objects are actually noise sources being mistakenly identified as a star by the SRU. SRU error messages were caused by moon occultations, stray light from the Earth, and elevated radiation in the South Atlantic Anomaly.*

is some residual stray light reaching the SRU optics, and this stray light accounts for the vast majority of the SRU reported errors.

Finally, the GNC team also observed that the SRU frequently reported the “excess stars” error condition over the South Atlantic Anomaly (SAA), which is the region over South America and the Atlantic Ocean where the Earth’s inner radiation belt dips closest to the Earth’s surface and the proton flux environment is higher than normal levels for a given orbital altitude. The red polygon plotted in Figure 11 shows the rough boundaries of the SAA as determined by the SMAP operations team. Although the SMAP spacecraft does not carry any type of traditional radiation detector, the SRU “excess stars” error condition has demonstrated sensitivity to the elevated radiation environment of the SAA. In a sense, the SRU reported errors act as a coarse and uncalibrated radiation detector akin to a low sensitivity Geiger counter. Again, it should be stressed that although the SRU reported error condition has produced an interesting data set to analyze, the error condition does not interfere with the ability of the SRU to produce inertial attitude estimates and the error condition does not interfere with the science operations of the spacecraft. The engineers on the operations team did make changes to the spacecraft FSW to more gracefully handle the SRU reported error condition, but this was due only to the distraction of the large number of errors – literally hundreds of thousands – being reported.

In flight, the SMAP SRU avionics have demonstrated sensitivity to sudden event upsets (SEUs) or radiation induced errors that have triggered multiple unplanned SRU resets. Four unplanned SRU resets have occurred as of Oct. 2015. However, following each reset the SRU immediately returned to normal operations after being commanded to acquire inertial attitude knowledge. Since the autonomous SRU resets were not anticipated prior to launch, the SMAP FSW initially responded to the SRU resets by safing the vehicle out of an abundance of caution. Two such safing events occurred. However, once the nature of the SRU resets was understood and had been confirmed through analysis and conversations with the SRU manufacturer, the SMAP FSW was changed so that unplanned SRU resets, of the experienced nature, are detected by the SMAP FSW and the SRU is automatically restored to normal attitude estimation without any interruption to science operations. As previously noted with the IRU, one lesson learned by the SMAP team as a result of the unplanned resets of both the IRU and SRU was the

need for the spacecraft flight software to have flexibility to allow for autonomous actions taken by GNC hardware components which contain their own CPU, software, and protection logic.

## V. Boom and Reflector Deployment and SPA Release

The SMAP spacecraft's outward appearance is dominated by the large reflector boom assembly (RBA) that is mounted to the top of the spun platform assembly (SPA). The 6 meter diameter deployable mesh reflector is attached to the end of the 5 meter long boom.<sup>10,11</sup> The boom has two segments and two hinges (Figure 1). The lower hinge, where the boom attaches to the base of the SPA is referred to as the shoulder joint, and the upper hinge, located midway up the boom between the SPA and reflector is referred to as the elbow joint.

The SPA, which includes the reflector, the boom, and all of the instrument electronics on the spinning portion of the spacecraft, was locked to the despun portion of the spacecraft at launch using multiple pyro separation nuts and an avionics cable originally connected the two spacecraft portions as well. At launch the reflector was packed tightly into a collapsed cylinder shape that was held shut with multiple pyro cables and was further fixed against the +X side of the spacecraft with a cradle (Figure 12). The boom in its launch configuration is also visible in Figure 12.

The deployments of the RBA assembly and SPA consisted of three separate irreversible deployment activities, each of which consisted of one-time pyro firings.<sup>10,11,12,13</sup> First, during the Boom Deployment activity the antenna launch restraint cradle (Figure 12) was released and the boom was deployed until both the elbow and shoulder joints had securely locked into the configuration shown in Figure 1. Second, during the Reflector Deployment activity, pyro cables holding the mesh reflector antenna in the closed bundle seen in Figure 12 were released and spoolers used tension to retract cables to deploy the reflector until every one of the multiple bays of the reflector had locked into the configuration seen in Figure 1. Finally, during the SPA Release activity, multiple separation nuts holding the SPA locked to the despun-portion of the spacecraft were fired and a telemetry cable connecting the two halves of the spacecraft was cut; thereby freeing the SPA to rotate.

Pyro firings are violent events that can cause the GNC sensors to measure large rates or accelerations that could interfere with the attitude controller functionality. Additionally, the mechanical engineers responsible for deploying the reflector required that the GNC controller be *inactive* during the deployments in order to ensure that the reflector was not damaged by controller torques while the reflector was mid-deployment. For these reasons, the GNC controller was transitioned to an idle control mode for all of the major spacecraft deployment events. In the GNC idle mode, attitude estimation is performed but the attitude control functions are inactive, with the exception of the logic which forces the RWAs to continue spinning at a constant spin rate.

The use of the idle control mode during the deployments meant that the spacecraft attitude was uncontrolled, and the solar array's pointing could potentially drift away from the sun. In order to limit the amount of time that the solar arrays would be pointed away from the sun during the boom and reflector deployment activities, the GNC team preemptively loaded a 8.25 Nms angular momentum bias along the spacecraft Y-axis, which is the solar array pointing direction. This 8.25 Nms momentum bias was the largest steady-state angular momentum that the vehicle has experienced. The momentum bias, which was added with MTR firings

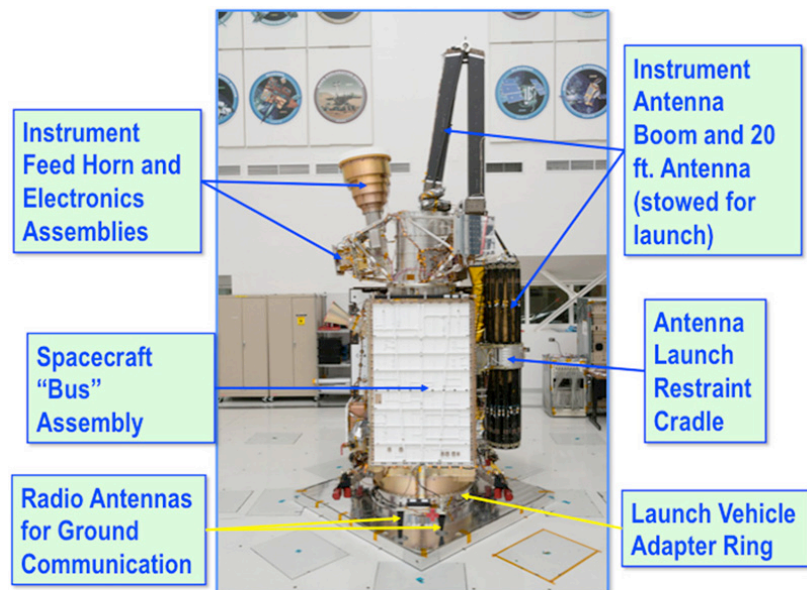


**Figure 12. SMAP Spacecraft in the Launch Configuration.** This image shows the SMAP spacecraft in the JPL cleanroom undergoing ground testing pre-launch. In the configuration shown, the SPA (spun platform assembly) is locked to the despun portion of the spacecraft, the two-segment boom is undeployed and the reflector is fixed to the +X panel of the spacecraft with the antenna launch restraint cradle. Image courtesy of the SMAP public webpage.<sup>1</sup>

over the course of 3 hours preceding the deployment activities, provided gyroscopic stiffness to the spacecraft Y-axis, thereby minimizing the amount that the solar arrays drifted away from pointing at the sun while the spacecraft controller was idle. The momentum bias used for the boom and reflector deployment proved effective. During the Boom Deployment activity, the attitude controller was idle for 16 minutes, and during this time the Y-axis drifted just 2.9 degrees from the Sun direction while the X and Z axis drifted by as much as 14.9 degrees. Similarly, during the 33 minutes that the controller was idle for the Reflector Deployment activity, the +Y axis was never more than 3.5 degrees from the Sun direction, even while the X and Z axes drifted by as much as 15.8 degrees.

No momentum bias was added for the SPA Release activity for two reasons: (1) the duration of time that the GNC controller was idle was shorter (just 6 minutes) than the idle periods for the boom and reflector deployments, and (2) the separation of the SPA was expected to produce primarily translational disturbances rather than rotational disturbances. The predictions were correct, and for the SPA Release activity, the spacecraft attitude drifted by only ~0.1 degrees.

The success of the Boom Deployment, Reflector Deployment, and SPA release activities were all confirmed in-flight by the operations team using micro-switches and tension sensors. However, pre-launch the operations team expended considerable effort to investigate the feasibility of using GNC sensor information as a backup data source

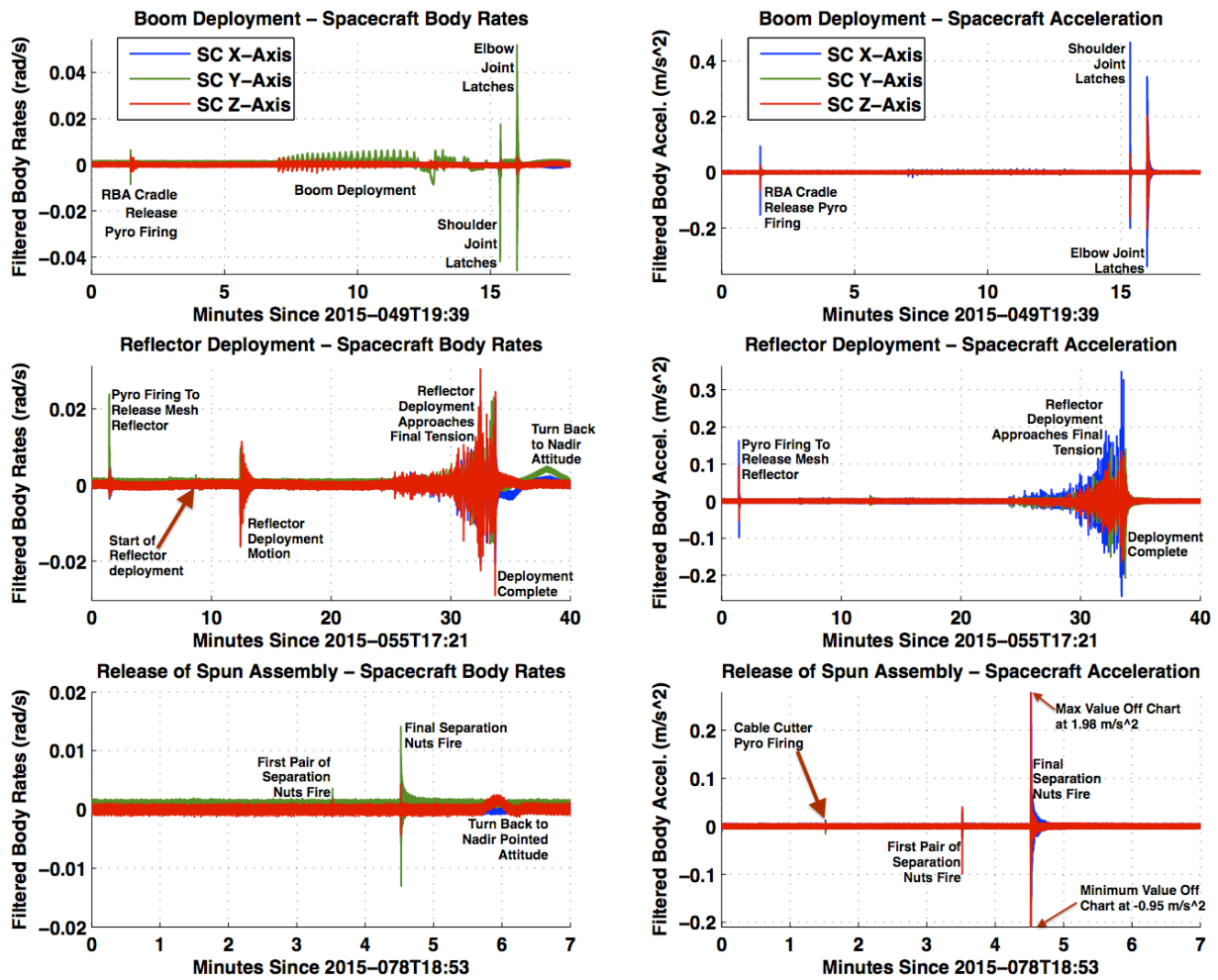


**Figure 13. IRU Rate and Acceleration Data During the Boom Deployment, Reflector Deployment, and SPA Release Activities.** These plots contain the high-rate (>100 Hz) IRU rate and acceleration data for each of the three major deployment events that occurred during the spacecraft commissioning. The accelerometer data shown in the right hand plots proved especially sensitive to the pyro firing events, while the motion of the boom and reflector during their deployments was best observed in the IRU body rate data. The high-rate IRU data was collected during each deployment and then downlinked after the deployment for ground processing and analysis. The IRU data provided independent confirmation that the deployment events had occurred nominally. Times are UTC.

in the event that any of the microswitches or tension sensors failed. Although the GNC controller was idle for each deployment, the IRU was nevertheless collecting high-rate ( $>100$  Hz) body rate and acceleration data for all three spacecraft axes, and this high-rate telemetry could be collected onboard as binary data and later downlinked for ground analysis. The high-rate IRU data is much higher resolution than the typical  $\frac{1}{2}$  Hz engineering telemetry, and is even faster than the 8 Hz control logic of the spacecraft. This made the high-rate IRU data the prime candidate for use to provide secondary confirmation of deployment success, albeit only after a lengthy delay required to downlink and process the recorded IRU data.

The IRU-A was easily able to detect every pyro-firing event that occurred during commissioning in the data from the accelerometers. The data from the IRU gyroscopes showed body rate transients for all but one pyro-firing. The high-rate body rate and acceleration data collected for the three major deployments is shown in detail in Figure 13. In this figure the left-hand plots contain the high-rate IRU gyroscope data while the right-hand plots contain the high-rate IRU accelerometer data. The figure is annotated so that the times of pyro firings and deployments are clear.

One interesting anecdote about the GNC performance during the deployment activities is in relation to the SPA Release activity. The first event to occur after the GNC controller transitioned to its idle state for the SPA Release activity was the firing of a pyro to cut a small cable that relayed temperature data between the spun and despun portions of the spacecraft. The cable cutter pyro firing, visible in the bottom right plot of Figure 13, produced the smallest acceleration and rate disturbances of any of the pyro events that occurred in the mission. Despite the small rate and acceleration disturbances, it is believed that the blast from the cable cutter pyro firing ejected a significant amount of particulate matter into the area surrounding the spacecraft. Within a few seconds of the cable cutter pyro firing the stellar reference unit (SRU) began to simultaneously report a higher than normal background noise level in the SRU images, the SRU also begun reporting instances of the “excessive number of stars detected” error described in section IV. G., and the number of real stars being tracked by the SRU also gradually decreased from 15 to 0. The apparent obstruction of the SRU field of view by the presumed cloud of sparkling particulate subsided gradually over the course of  $\sim 6$  minutes. The SRU interference from the cable cutter firing was not anticipated, but it also did not interfere with GNC performance since the GNC controller was idle during this period anyhow. It is unknown whether the SRU would have encountered similar particulate obstruction during the Boom and Reflector Deployment activities because the SRU was manually commanded to suspend attitude estimation during those activities to avoid potential issues if the SRU were to be obstructed by the Earth.

## VI. $\Delta V$ Maneuver Performance

The Delta II launch vehicle intentionally injected SMAP into an initial orbit which was  $\sim 11$  km lower and also more eccentric than the final planned science orbit. Therefore, the mission plan always included several  $\Delta V$  maneuvers using the RCS thrusters to reach the desired spacecraft science orbit. In all, the SMAP commissioning plan included opportunities for 10 planned maneuvers, though half of those would only be needed in the event of “worst case” launch vehicle injection errors. However, following launch, the NAV team determined that there was no need to execute the majority of the maneuvers, and they were removed from the commissioning plan.

For the SMAP mission, the NAV team specifies the required maneuver  $\Delta V$  vector as a fixed vector in an orbit relative frame. Note that the  $\Delta V$  vector is *not* an inertially fixed vector. The  $\Delta V$  vectors specified by the NAV team are defined relative to the RTN frame, where “R” is the radial vector from the center of the Earth to SMAP, “N” is the vector that is normal to the SMAP orbital plane, and “T” is the transverse vector that is nearly in the orbit velocity direction and completes the right handed RTN coordinate frame. To execute a prograde maneuver (i.e. one that is roughly in the orbit velocity direction) and increase the orbital energy, the SMAP spacecraft pitches  $+90$  degrees around the spacecraft  $+Y$  axis so that the  $+Z$  axis is aligned with the  $+T$  axis of the RTN frame. Retrograde maneuvers require a pitch of  $-90$  degrees around the  $+Y$  axis. Both prograde and retrograde maneuvers keep the solar arrays pointed at the sun, so there is no interruption to power collection and there are no large thermal transients due to solar heating during the maneuver. Maneuvers to change the spacecraft inclination could theoretically be accomplished by simply rolling the spacecraft  $\pm 90$  around the spacecraft X-axis so that the Z-facing thrusters are aligned with the  $+N$  or  $-N$  direction in the RTN frame. However, in order to avoid violating thermal constraints, the SMAP spacecraft uses a more complicated maneuver attitude for inclination maneuvers, where the spacecraft  $+Z$  is still exactly aligned with the  $+N$  or  $-N$  direction, but the spacecraft is clocked around that burn direction in order to minimize the angle between the sun and solar arrays. In general, this maneuver attitude definition will require turns larger than  $90$  degrees because there are rotation components around all three axes. In

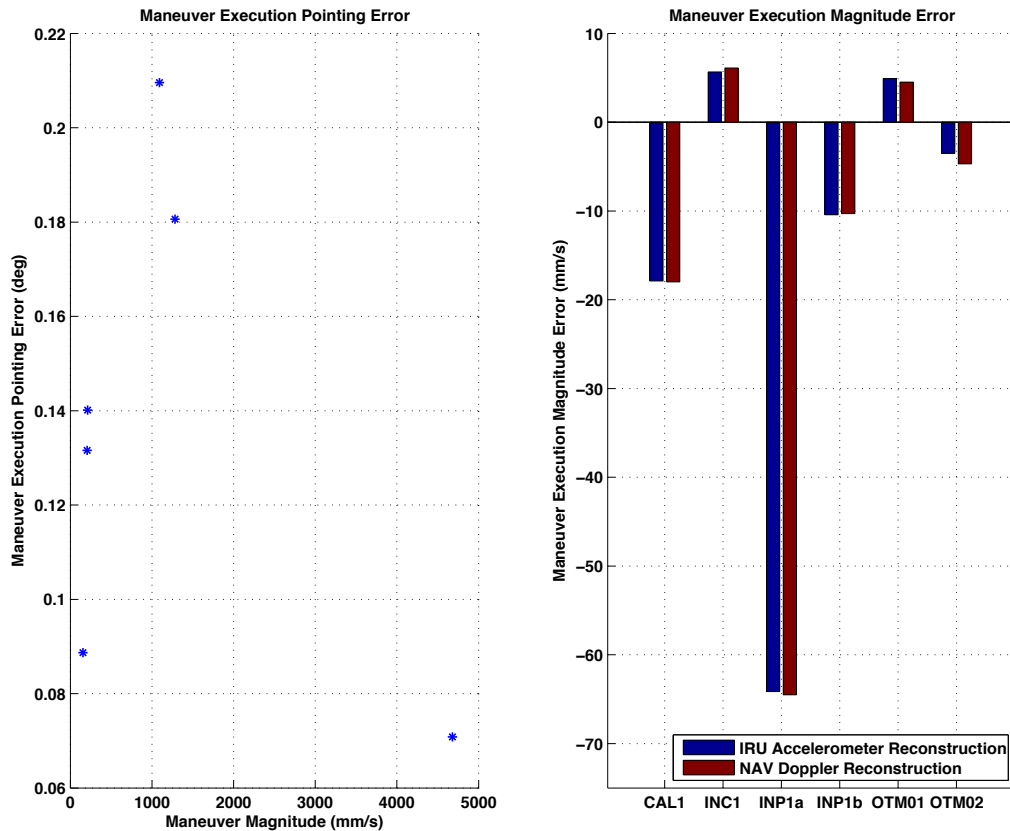


**Figure 14. SMAP Maneuver Execution Errors.** *The maneuver execution pointing error is shown as a function of the total maneuver magnitude in the left plot. The pointing error is expressed as a percentage of the total maneuver magnitude, and is in a direction perpendicular to the burn direction. The execution error in the right-hand plot is shown for all 6 of the executed SMAP maneuvers. Maneuver magnitude error is execution error in the direction of the desired burn direction. Positive values represent over-burns and negative values reflect under-burns. The GNC reconstruction based on accelerometer integration is compared to the Navigation team’s Doppler reconstruction. NAV and GNC reconstruction agree within 1.2 mm/s for all maneuvers.*

principle SMAP could execute a maneuver where the RTN  $\Delta V$  vector has non-zero components in multiple axes. However, the NAV team did not request any such maneuver during the spacecraft commissioning.

SMAP maneuvers are “timed burns” where the spacecraft is provided with the desired burn magnitude and fixed parameters for the spacecraft mass, expected RCS thrust magnitude, and expected thruster ISP. The GNC flight software will then determine the total amount of thruster on-time required to produce the commanded  $\Delta V$ . As previously described in section IV.B, the SMAP IRU includes accelerometers in addition to the gyros. Despite the presence of working accelerometers in the IRU, the GNC flight software does not use the accelerometer data anywhere in the GNC algorithms because the SMAP project did not need accelerometer data in order to meet maneuver execution accuracy requirements. Despite the fact that the GNC flight software architects chose not to make use of the available accelerometer data in their algorithms, the GNC operations team readily accepted this additional dataset, which can be used to reconstruct the executed maneuver magnitude. The GNC operations team has collected high-rate IRU accelerometer data for every SMAP maneuver and the GNC estimated maneuver execution error (Figure 14) never differ from the Navigation team’s Doppler reconstruction by more than 1.2 mm/s.

The GNC  $\Delta V$  control logic was designed so that maneuvers can be performed regardless of whether the SPA is spinning or not, but the least stressful case for the GNC  $\Delta V$  controller was to perform maneuvers with the boom and reflector deployed, but with the SPA still locked to the despun portion of the spacecraft. For this reason, the commissioning maneuvers were scheduled to occur after the Boom Deployment and Reflector Deployment activities had completed, but before the SPA Release activity occurred. After the completion of the SMAP commissioning, the spacecraft also demonstrated the ability to perform maneuvers with the SPA spinning with two orbit maintenance maneuvers.

During commissioning, SMAP executed four maneuvers which were named: CAL1, INC1, INP1a, and INP1b. After commissioning was complete, and regular maintenance of the science orbit began, SMAP also executed OTM01 and OTM02. The accuracy of the executed maneuvers can be determined by examining the execution error. For SMAP, the maneuver execution error is divided into two components. The magnitude error component is the difference between the commanded and achieved  $\Delta V$  vector in the direction of the commanded  $\Delta V$  vector, where positive magnitude errors represent over-burns and negative magnitude errors represent under-burns. The angular distance between the commanded and achieved  $\Delta V$  vectors defines the pointing error of the executed maneuver. The execution errors for all maneuvers executed by SMAP are shown in Figure 14. Since the absolute maneuver execution error magnitude is plotted in Figure 14, it is expected that larger maneuvers (i.e. CAL1 and INP1a) will have larger magnitude errors, though proportionally, the execution error magnitude was never larger than 3% of the commanded maneuver magnitude.

There was a specific purpose for each of the commissioning maneuvers. The 1.28 m/s CAL1 maneuver, was performed in the +T direction of the RTN frame, but the primary purpose of the maneuver was to verify the stability and effectiveness of the  $\Delta V$  GNC control mode, validate the models used to predict the RCS duty cycling behavior, and, most importantly, to calibrate the effective thrust from the RCS thrusters. The INC1 maneuver was the only inclination maneuver that SMAP has executed and was a 206 mm/s maneuver in the -N direction. The INC1 maneuver and the Low Rate Spinup activity were the only commissioning activities that intentionally turned the spacecraft to an attitude that was not power positive. INP1a was the largest maneuver executed to date at 4.68 m/s, and was executed in the +T direction to raise perigee to the desired orbital altitude. The INP1b maneuver was the only retrograde maneuver executed to date and was 1.09 m/s in magnitude executed in the -T direction and was used to circularize the SMAP orbit by decreasing the apogee altitude. For navigation reasons, the INP1a and INP1b maneuvers were required to be executed as close together in time as possible, and they were therefore executed on the same day just 1.5 orbits apart from one another. After the completion of the INP1a and INP1b maneuvers, SMAP reached its final science orbit and only small orbit maintenance burns are now required. The OTM01 and OTM02 maneuvers were small maneuver of 212 mm/s and 156 mm/s respectively, performed in the +T direction of the RTN frame. OTM01 was the first maneuver to occur while the SPA was spinning at 14.6 rpm and demonstrated that the GNC  $\Delta V$  controller performs as expected with the SPA spinning.

## VII. The Low Rate Spinup and High Rate Spinup Activities

After the completion of the deployment activities and after the spacecraft had performed maneuvers to reach the final science orbit, the last major engineering activity in the spacecraft commissioning was the spinup of the SPA to the 14.6 rpm science spin rate. The spacecraft bus and SPA are connected to each other by the Bearing and Power Transfer Assembly (BAPTA). The BAPTA is the motor used to spin the SPA and the BAPTA also carries both power and telemetry across the spin bearing. For the SMAP science mission, the BAPTA is designed to control the SPA rotation rate for commanded spin rates between 5-14.6 rpm, but the BAPTA is unable to sustain controlled spin-rates below 5 rpm. As a result, the spinup of the SPA from 0 rpm to 14.6 rpm must be performed in separate activities: the Low Rate Spinup activity is used to spinup the SPA from 0 rpm to 5 rpm, and High Rate Spinup activity slowly accelerates the BAPTA spin-rate from 5 rpm to 14.6 rpm over the course of ~80 minutes. Both the Low Rate and High Rate Spinup activities are described in detail in this section.

### H. Low Rate Spinup Activity

In the Low Rate Spinup activity the BAPTA accelerates from 0 to 5 rpm in just 80 seconds. As the BAPTA applies torque to spinup the 234.7 kg-m<sup>2</sup> SPA to 5 rpm, the spacecraft body receives an identical torque in the opposite direction which far exceeds the maximum control torque available from the RWA controller, and the spacecraft is forced to tumble around the Z-axis. This behavior was anticipated early in the design of the spacecraft, so the GNC flight software includes a Low Spin Control Mode, which is a mode in which the RWA controller only attempts to reduce spacecraft body rates, without any effort to control spacecraft attitude. The Low Spin Control Mode can therefore be considered a “detumble” mode, and only after the Low Spin Control Mode has sufficiently nulled the spacecraft body rates will the spacecraft transition to the High Spin Control Mode to control both spacecraft attitude and rates while spinning.

The detumbling of the spacecraft in the Low Spin Control Mode is accomplished on RWA control, so there is no significant change to the system angular momentum during the spinup activity. Before the spinup, the spacecraft is in a zero momentum state, and then while the spacecraft is tumbling (after the BAPTA spinup) the net momentum of the SPA at 5 rpm and the tumbling spacecraft body still sum to ~0 Nms. Finally, after the RWA controller has finished detumbling the spacecraft, the SPA spun momentum is exactly countered by the angular momentum of the

reaction wheels resulting in a net angular momentum of  $\sim 0$  Nms. To add further emphasis to this point: the RCS thrusters are *not* used to spinup the SPA because doing so would expend consumables and add a large inertial angular momentum to the system that would then need to be removed.

The telemetry from the Low Rate Spinup Activity is shown in Figure 15. In these plots the first vertical magenta line denotes the time that the spacecraft entered the Low Rate Control mode and began the spinup activity, and the second vertical magenta line denotes the time that the RWA controller had succeeded in nulling spacecraft body rates and the spacecraft transitioned to the High Spin Control Mode. After the SPA began to spinup to 5 rpm, the spacecraft was forced into a tumble (Figure 15) around the Z-axis which achieved a peak body rate of 0.19 rad/s (11 deg/s), which is the fastest that the spacecraft has rotated in flight. The close inspection of the +Y to Sun angle in the top right plot in Figure 15 shows that during the 4 minutes while the spacecraft was tumbling, it completed 3.5 revolutions of counter-rotation before the RWA controller successfully nulled the tumble. After the detumbling is complete and the spacecraft transitioned to the High Rate Spinup control mode the spacecraft executed a large 159 degree slew around the Z-axis to return the spacecraft to the normal nadir pointed attitude.

During the Low Rate Spinup the spacecraft reaches the largest rotation rates it sees at any phase of the mission. De-spinning the SPA would cause the spacecraft to tumble in the same manner, though this has never been tested in flight. For these reasons, the Low Rate Spinup activity is regarded as a stressful scenario for the spacecraft, and one that the operations team avoids repeating if possible. To avoid the need to frequently spinup or spin down the spacecraft, the majority of the fault protection (FP) monitors keep the SPA spinning at the current spin rate, even in cases where the vehicle transitions to a safe mode. Only in cases where there is a BAPTA fault or severe GNC attitude control fault will the SPA be spun down as part of the safing response. Barring some unforeseen anomaly, there are no plans to intentionally spin down the SPA at any point in the mission.

The Low Rate Spinup activity also provided the GNC team with the first opportunity to make an in-flight measurement of the Izz inertia of the SPA (the Z-axis inertia of the spun portion of the spacecraft). The GNC team

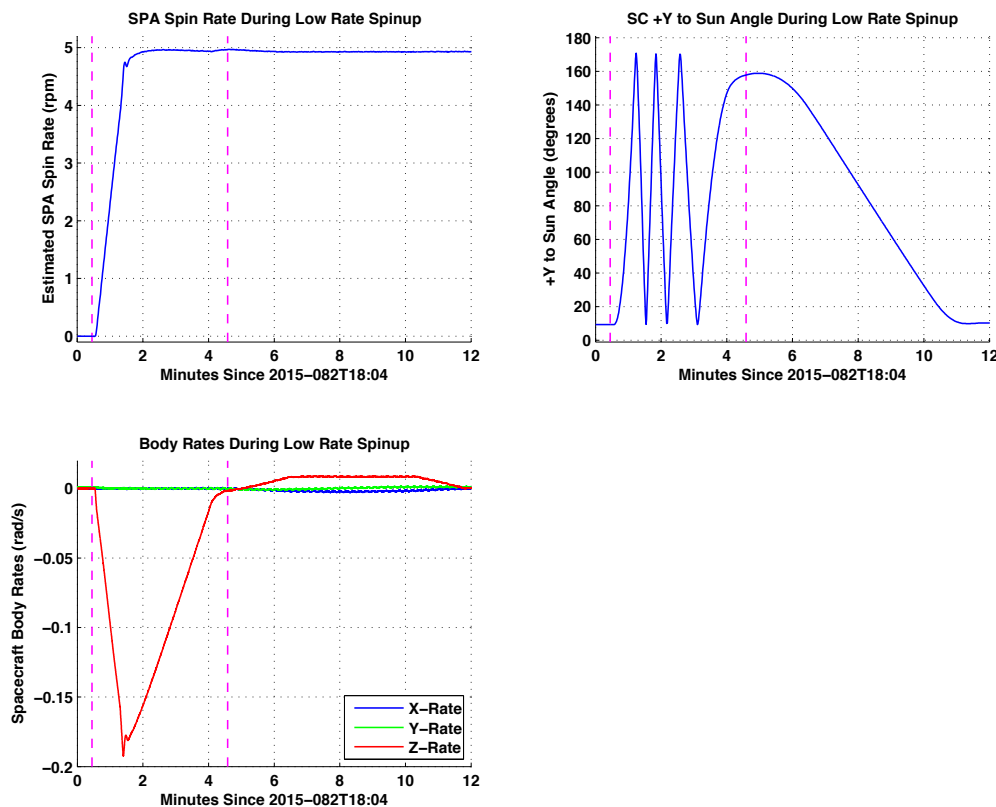


**Figure 15. GNC Telemetry for SPA Spin Rate, +Y to Sun Angle, and Spacecraft Body Rates During the Low Rate Spinup Activity.** The GNC telemetry included in these plots show the SPA spinning-up from 0 to 5 rpm in  $\sim 80$  seconds, and the total time required for the RWA controller to regain control of the tumbling spacecraft (the period between the two vertical magenta lines) was 4 minutes. During the Low Rate Spinup, the spacecraft reached peak body rate of 0.19 rad/s and the tumbling resulted in 3.5 revolutions of counter rotation before the RWA controller nulled the tumbling. Times are UTC.

found that the SPA had an Izz inertia that was  $4.0 \text{ kg}\cdot\text{m}^2$  smaller than predicted pre-launch. This inertia mismatch was well within the range of uncertainty for the fully deployed boom and reflector, which could not undergo integrated mass property testing in a 1G environment.

### I. High Rate Spinup Activity

The High Rate Spinup activity finished the process of accelerating the SPA from 5 rpm to 14.6 rpm. Note that High Rate Spinup activity does not need to occur immediately after the completion of the Low Rate Spinup activity. In fact, during the SMAP commissioning, 3 days elapsed between the completion of the Low Rate Spinup activity and the beginning of the High Rate Spinup activity. However, only a subset of spacecraft activities is possible while the spacecraft is at the 5 rpm intermediate spin rate.

Once the SPA spin rate reaches 5 rpm, the BAPTA is able to control and make fine adjustments to the SPA spin rate. Therefore it is possible for the operations team to profile a very gradual SPA spinup from 5 to 14.6 rpm that requires 80 minutes to complete. The BAPTA torque required to produce this small SPA acceleration is less than the available RWA control torque, meaning that it is possible for the RWA controller to maintain attitude control and keep the spacecraft at the nadir attitude through the spinup from 5 to 14.6 rpm. The BAPTA hardware can spin faster than 14.6 rpm and the GNC controllers would be able to tolerate a spin rate as high as 14.8 rpm without exceeding the limits of the momentum budget. However, the 14.6 rpm spin rate was selected pre-launch by the mission planners as the optimal spin rate at SMAP's orbital altitude to maximize the quantity and quality of data collected by the radar and radiometer. For that reason, there are no plans to ever spin the SPA at any spin rate other than 14.6 rpm.

The SPA was designed to be balanced with its center of mass along the spin axis when the boom and reflector

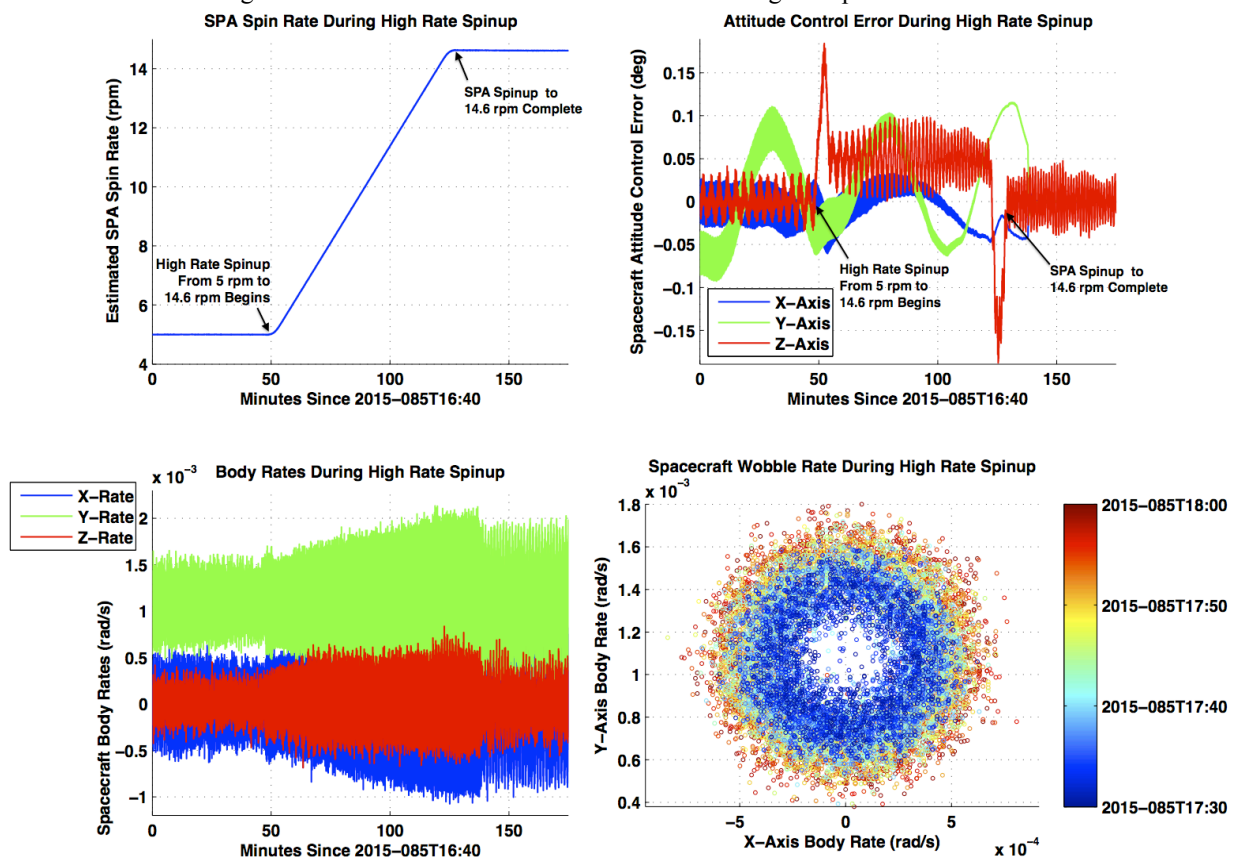


**Figure 16. GNC Telemetry for SPA Spin Rate, Attitude Error, and Spacecraft Body Rates During the High Rate Spinup Activity.** The GNC telemetry included in these plots show the SPA spinning-up from 5 to 14.6 rpm in ~80 minutes (top left). The top right plot shows that during the spinup, the RWA controller maintained spacecraft nadir pointing to better than 0.2 degrees of attitude error. The bottom two plots show the spacecraft body rates as a function of time on the left, and the X-rate vs. Y-rate on the right. The bottom right hand plot, demonstrates the increasing size of the wobble rate as the SPA rate increases (i.e. the radius of the wobble circle grows). Times are UTC.

are in their fully deployed configuration.<sup>10,11,14</sup> However, the GNC flight software design always included provisions for the inevitable spacecraft wobble that results from an X or Y axis offset between the SPA center of mass and the spin axis. The SMAP spacecraft mechanical structure and balancing was designed to produce a wobble angle smaller than 0.5 degrees when the SPA is rotating at 14.6 rpm, and the GNC attitude controller is designed to function without any performance degradation for wobble angles up to 0.5 degrees.<sup>14</sup> The “wobble angle” is just the rss of the unfiltered X and Y axis attitude control error components. The SMAP mission pointing requirements for the RWA controller during science operations require that the absolute attitude control errors be less than  $[X, Y, Z] = [0.1, 0.1, 0.28]$  degrees 3-sigma. The requirement excludes wobble induced pointing error, so the controller is not required to try to fight or control the higher frequency spacecraft wobble. The spacecraft body rates are required to be less than 0.070 rad/s per axis 3-sigma excluding wobble induced rates. To meet the pointing requirements, the GNC controller uses a double notch filter that is tuned to filter out all oscillations in the body rate and attitude control error data at frequencies near 0.243 Hz, which corresponds to the 14.6 rpm spin rate, with a second notch at the first harmonic. The notch filter frequencies are fixed parameters that do not vary as a function of SPA spin rate. As a result, the RWA controller is designed to meet science pointing requirements when the SPA is spinning at 14.6 rpm, but if the SPA spin rate is any other value, then the RWA controller will be fighting to control the spacecraft wobble which is outside the bandwidth of the RWA controller. For this reason, the GNC flight software includes two RWA control modes with different gain sets; one is the High Spin Rate RWA Control mode which has looser gains and allows larger pointing errors and rate errors for cases where the SPA spin rate is somewhere between 5-14.6 rpm. This control mode is used only when the SPA is in the process of being spun up to 14.6 rpm. The second RWA control mode is the standard RWA pointing mode used for precise spacecraft pointing when the SPA spin rate is exactly 0 rpm or 14.6 rpm.

Flight telemetry for the High Rate Spinup activity is shown in Figure 16. The plotted data shows the SPA spin-rate gradually increasing from 5 to 14.6 rpm in a smooth and continuous manner. The attitude control error plotted in Figure 16 shows that the spacecraft maintained the nadir pointed attitude to better than 0.2 degrees throughout the entire spinup from 5-14.6 rpm. The effectiveness of the RWA controller notch filter can be seen by careful examination of the X and Y axis attitude errors (blue and green) in the top right plot of Figure 16. In that plot the variance or noise level of the X and Y attitude errors decreases dramatically as the SPA spin rate approaches the 0.243 Hz notch filter frequency. The body rate data plotted in the bottom left of Figure 16 shows the increased noise magnitude as the spin-rate increases and the wobble frequency therefore increases. Plotting the estimated X-axis body rate vs. the Y-axis body rate traces out circles where the radius is the wobble rate, which grows as a function of time during the spinup activity.

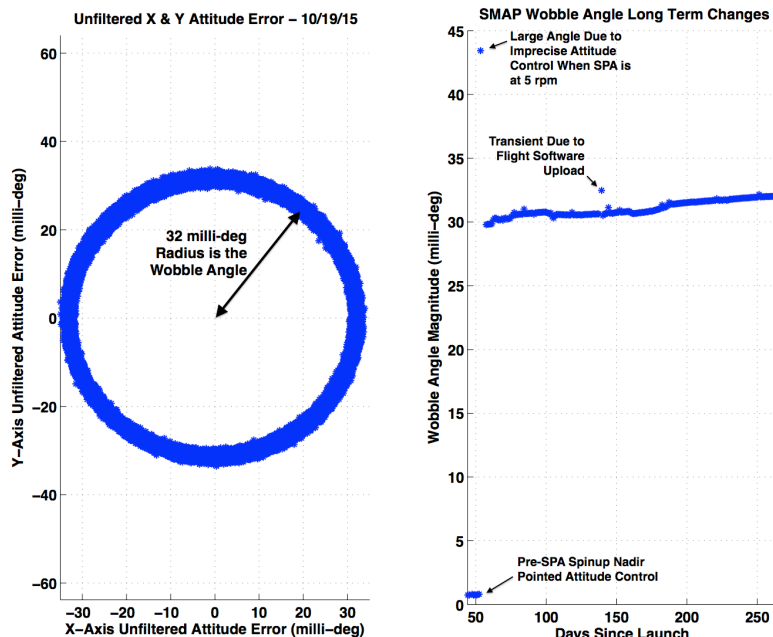


**Figure 17. Spacecraft Wobble Angle History.** The left plot shows the unfiltered X-axis vs. Y-axis attitude error during a typical 24 hour period of nadir pointed science operations with the SPA spinning at 14.6 rpm. The circular trace is wobble due to an offset between the SPA center of mass the spin axis. The right plot shows the daily average estimated wobble angle over the course of the mission. The wobble angle has shown slow secular growth from 29.8 milli-deg shortly after the High Rate Spinup activity to 32.0 milli-deg in Oct. 2015

After the SPA spinup to 14.6 rpm was complete and the GNC control mode was transitioned to the normal RWA control mode used for science operations, the X and Y axis attitude control errors are 0 mean value with a standard deviation of 0.5 milli-deg, with peak attitude errors of just 2.0 milli-deg, which is 50x better than the required value. The Z-axis attitude error is dominated by a 70 second period BAPTA bearing harmonic that results in a Z-axis attitude error that is still 0 mean value but has a 22.2 milli-

deg standard deviation, and peak values of ~60 milli-deg. The Z-axis attitude error is still ~5x better than the requirement.

Although the reaction wheel control logic uses filtered attitude and rate information in order to achieve science pointing, the unfiltered rate and attitude telemetry are still available in telemetry for ground analysis. The X and Y axis unfiltered attitude control error channels are especially useful for observing the real time spacecraft wobble angle, as shown in Figure 17. In the left plot of Figure 17, the X-axis unfiltered attitude error is plotted against the Y-axis unfiltered attitude error for 24 hours of telemetry from Oct 19, 2015. The unfiltered attitude error traces out the circular shape due to wobble induced by the non-zero offset between the SPA center of mass the spin axis. The circular shape in Figure 17 is actually slightly elliptical, with a peak X-axis wobble angle of 33.0 milli-deg and a peak Y-axis wobble angle of 31.6 milli-deg. The average wobble angle during the period of time plotted is 32.0 milli-deg.

The wobble angle computed from the rss of the unfiltered X and Y attitude control errors is a quantity that has been computed and trended since the SPA spinup activity was performed. Interestingly, there has been a long term secular growth in the spacecraft wobble angle from 29.8 to 32.0 milli-deg over the course of 200 days of nadir pointed operations with the SPA at 14.6 rpm. The growth in the wobble angle was not anticipated and is hypothesized to be due to slight thermal expansion/contraction of the reflector and boom based on seasonal changes in sun illumination angle. While the long term change in the wobble angle is a curiosity, it does not present any threat to GNC controller performance since the GNC controller was designed to function in the presence of a wobble angle as large as 500 milli-deg; a factor of 17x more than the current wobble angle. Overall the attitude controller performance since the completion of the High Rate Spinup activity has been excellent, working exactly as designed.

## VIII. Conclusion

Today the SMAP spacecraft is quietly circling the Earth and beaming back global soil moisture measurements<sup>16</sup> with almost no involvement from the operations team; day to day operations are almost fully automated at this point.<sup>17</sup> There is very little evidence that just a few months ago the SMAP operations team was in the thick of a complex and challenging commissioning phase in which countless operations activities needed to be successfully accomplished to checkout the GNC hardware and software functionality and phasing, deploy the boom and reflector, spinup the spacecraft to the desired science spin rates, and perform  $\Delta V$  maneuvers to move SMAP to the final science orbit. All of the required GNC tasks that were a part of the spacecraft commissioning were successfully executed and all GNC hardware and software continue to function nominally. The spacecraft commissioning period included multiple minor GNC anomalies which provided interesting challenges for the operations team, but none have caused anything but short term interference with normal science operations. The GNC subsystem on the SMAP spacecraft is currently healthy and ready to support a long science mission of Earth observations.

## Acknowledgments

The research described in this paper was carried out at the Jet Propulsion Laboratory, California Institute of Technology, under contract with the National Aeronautics and Space Administration. Copyright 2015 California Institute of Technology. Reference to any specific commercial product, process, or service by trade name, trademark, manufacturer, or otherwise, does not constitute or imply its endorsement by the United States Government or the Jet Propulsion Laboratory, California Institute of Technology. U.S. Government sponsorship acknowledged.

The author would like to recognize the members of the SMAP GNC Operations team, including Shawn Johnson, Matt Wette, and Daniel Eldred. All results shown in this paper are due to the efforts of the full GNC Operations team. It was a pleasure and honor to lead such a talented and organized subsystem through SMAP's commissioning. I also want to recognize Bryan Kang, who provided excellent leadership for the GNC subsystem throughout the spacecraft development and served as the Commissioning Phase lead for the project. Credit is also owed to the GNC Control Analysis team, the GNC Hardware team, and the SMAP Flight Operations Team who are too numerous to list here. Their collective knowledge was a tremendous asset during the spacecraft commissioning. Finally, I want to thank Tina Sung who helped in reviewing this paper, and who will now take the GNC reigns on SMAP.

## References

<sup>1</sup>JPL SMAP website: <http://smap.jpl.nasa.gov>.

- <sup>2</sup>“Soil Moisture Active Passive Launch Press Kit,” NASA/JPL, January 2015, URL: [http://www.jpl.nasa.gov/news/press\\_kits/smaplaunch.pdf](http://www.jpl.nasa.gov/news/press_kits/smaplaunch.pdf)
- <sup>3</sup>Entekhabi, D., E. Njoku, P. O'Neill, K. Kellogg et al., "The Soil Moisture Active Passive (SMAP) Mission," *Proceedings of the IEEE*, vol. 98, no. 5, May 2010.
- <sup>4</sup>“SMAP Handbook Soil Moisture Active Passive Mapping Soil Moisture and Freeze/Thaw from Space,” NASA/JPL, July 2014, URL: [http://smap.jpl.nasa.gov/system/internal\\_resources/details/original/178\\_SMAP\\_Handbook\\_FINAL\\_1\\_JULY\\_2014\\_Web.pdf](http://smap.jpl.nasa.gov/system/internal_resources/details/original/178_SMAP_Handbook_FINAL_1_JULY_2014_Web.pdf)
- <sup>5</sup>Entekhabi, D.; Njoku, E.G.; Houser, P.; Spencer, M.; Doiron, T.; Yunjin Kim; Smith, J.; Girard, R.; Belair, S.; Crow, W.; Jackson, T.J.; Kerr, Y.H.; Kimball, J.S.; Koster, R.; McDonald, K.C.; O'Neill, P.E.; Pultz, T.; Running, S.W.; Jiancheng Shi; Wood, E.; Van Zyl, J., "The hydrosphere State (hydros) Satellite mission: an Earth system pathfinder for global mapping of soil moisture and land freeze/thaw," in *Geoscience and Remote Sensing, IEEE Transactions*, vol.42, no.10, pp.2184-2195, Oct. 2004.
- <sup>6</sup>O'Neill, P, Entekhabi, D., Njoku, E., Kellogg, K., "The NASA Soil Moisture Active Passive (SMAP) Mission: Overview." *Geoscience and Remote Sensing Symposium (IGARSS), 2010 IEEE International*, IEEE, 2010.
- <sup>7</sup>“SMAP Team Investigating Radar Instrument Anomaly,” NASA/JPL, August 5, 2015, URL: <https://www.nasa.gov/jpl/smap-team-investigating-radar-instrument-anomaly>
- <sup>8</sup>“NASA Soil Moisture Radar Ends Operations, Mission Science Continues,” NASA/JPL, September 2, 2015, URL: <http://smap.jpl.nasa.gov/news/1247/>
- <sup>9</sup>“Earth Science and Applications from Space: National Imperatives for the Next Decade and Beyond,” *Committee on Earth Science and Applications from Space: A Community Assessment and Strategy for the Future*, National Research Council, The National Academic Press, 2007.
- <sup>10</sup>Eremenko, A., Kastner, J., Hoffman, P., “SMAP Observatory Configuration, from Concept to Preliminary Design,” *Proceedings of the 2010 IEEE Aerospace Conference*, Big Sky, MT, USA, March 6-13, 2010.
- <sup>11</sup>Eremenko, A., Kastner, J., “SMAP Observatory Concept – A Configuration of Compromises,” *2011 IEEE Aerospace Conference*, Big Sky, MT, USA, March 5-12, 2011.
- <sup>12</sup>Mobrem, M., Keay, E., Marks, G., Slimko, E., “Development of the Large Aperture Reflector/Boom Assembly for the SMAP Spacecraft,” *ESA/ESTEC Workshop on Large Deployable Antennas*, Noordwijk, Netherlands, 2-3 Oct, 2012.
- <sup>13</sup>Mobrem, M., S. Kuehn, C. Spier, and E. Slimko, "Design and Performance of Astromesh Reflector Onboard Soil Moisture Active Passive Spacecraft," *IEEE 2012 Aerospace Conference*, March 2012.
- <sup>14</sup>Alvarez-Salazar, O. S., D. Adams, M. Milman, R. Nayeri, S. Ploen, L. Sievers, E. Slimko, and R. Stephenson, "Precision Pointing Architecture of SMAP's Large Spinning Antenna," *Proceedings of AIAA Guidance, Navigation and Control (GNC) Conference*. Vol. 19. Boston, MA, USA AIAA, 2013.
- <sup>15</sup>Murray, A., Jones, C.G., Reder, L., Cheng, S., “The Use of Modeling for the Flight Software Engineering on SMAP,” *IEEE 2011 Aerospace Conference*, March 2011.
- <sup>16</sup>Yueh, S., Entekhabi, D., Kellogg, K., O'Neill, P., Njoku, E., “Early Results from NASA Soil Moisture Active Passive Mission,” *SMOS Science Conference*, 28 May, 2015.
- <sup>17</sup>Sanders, A., “Automating the SMAP Ground Data Systems to Support Lights-Out Operations,” *SpaceOps Conferences 2014*, Pasadena, CA, 5-9 May, 2014, AIAA 2014-1781.